DOE/ER/60233--T1

DE92 007126

Department of Energy
DOE DE-FG03-84ER60233

1991 ANNUAL REPORT

"Radioimmunotherapy: Development of an Effective Approach"

Sally, J. DeNardo, M.D.
Principal Investigator

Gerald L. DeNardo, M.D.
Co-Principal Investigator

Claude F. Meares, Ph.D.
Co-Principal Investigator

University of California, Davis
Department of Internal Medicine
Division of Hematology/Oncology
Section of Radiodiagnosis/Therapy

SUMMARY ABSTRACT

Our group has already demonstrated substantial regression of B cell lymphoma and leukemia using Lym-1 monoclonal antibody labeled with ^{131}I. Complete remissions were achieved. Those obtained at higher radiation dose rates have generally been more prolonged with some at 1-2 years at present.

We plan to extend our success in treating B cell malignancies with ^{131}I labeled Lym-1 by a major effort in therapy with ^{67}Cu Lym-1, which has been pioneered by this D.O.E. program. Our recent pharmacokinetics and early therapeutic responses with this radiopharmaceutical substantiate our previous projections that ^{67}Cu could offer a therapeutic advantage in treating lymphoma and other cancers. We have recently requested the supplement necessary to support the ^{67}Cu special costs which will be incurred beyond the portion funded by this budget.

Yttrium-90, labeled by a macrocycle, DOTA will be studied in patients as a continuation of the ^{111}In-BAD (DOTA) Lym-1 studies reported in this annual report. Excellent images and pharmacokinetics of the ^{111}In-BAD(DOTA)-Lym-1 encourage us to initiate the combined $^{90}Y/^{111}In$-BAD(DOTA)-Lym-1 studies. Lymphomas and related diseases represent a special case for radioimmunotherapy because of their documented radiosensitivity and immunodeficiency, and thus offer a unique opportunity to conduct therapeutic feasibility studies in a responsive human model.

Using murine and chimeric L6 and other MoAb to breast cancer, we have applied the strategies that were developed in taking Lym-1 antibody from the bench to the patient. We have examined a number of monoclonal antibodies for treatment of breast cancer and chose chimeric L6 for prototype studies because of certain characteristics. Reasons for selecting L6 were its similarity to Lym-1 and its tumor cell cytotoxicity in vitro. After pharmacokinetic studies with ^{131}I Ch L-6 were completed, therapy studies in 11 patients revealed clinical response in 6. Several other promising MoAbs, including one that internalizes into the cancer cell, are under investigation because they offer additional therapeutic or mechanistic opportunities. Breast cancer is different from B cell malignancies because immunodeficiency is less likely, the tumor cells are less radiosensitive, and antigen targets are generally less homogeneous. This provides opportunities to explore differences and similarities. Breast cancer is more common than B cell malignancies, but shares with B cell malignancies no current hope of curative therapy after initial metastasis. It should be noted that most of the antibodies we are using for breast cancer also target prostate cancer and lung cancer.

The chemistry of attachment of conjugates to antibodies and their impact on immunological targeting and biological activities (cytotoxicity), metabolic fate, and therapeutic index will continue to be a major strength and function of this program. From the beginning, this grant has supported the conception, synthesis, and development of the first macrocylic, bifunctional chelating agent TETA (6-p-nitrobenzyl-1,4,8,11-tetraazatetradecane-N,N',N",N"'-tetraacetic acid and its derivatives, including Lym-1-2IT-BAT), for use in Cu-67-based radioimmunodiagnosis and therapy. This work has led to the further devlopment of several new macrocylic bifunctional chelating agents for copper, indium, yttrium and other metals.

Radiometal Labeling of Lym-1 Conjugates. Successful Cu-67 labelings of Lym-1-2IT-BAT for human radiopharmaceutical have shown patient pharmacokinetics of ^{67}Cu-BAT(TETA)-Lym-1 with promising therapeutic dosimetry.

$^{111}In/^{90}Y$ BAD(DOTA)-Lym-1. ^{111}In-BAD(DOTA)-Lym-1 has recently been studied in 4 patients with excellent tumor uptake and good excretion of ^{111}In (reported here). The combined $^{111}In/^{90}Y$ DOTA Lym-1 studies will now be initiated in patients in an MTD for therapy. ^{111}In-BAD(DOTA)-Ch L-6 studies have been done in mice and the IND for breast cancer patients is in progress. Radioautography of mice receiving ^{90}Y-BAD(DOTA)-Lym-1 demonstrate no bone uptake and excellent tumor uptake (see Illustration in this report).

Several positron-emitting radiometals, among them Ga-68 Cu-64 and Mn-52, are expected to form stable chelates with one or more macrocycle chelating agents. Binding studies have been conducted using the longer lived isotopes Ga-67 and Mn-54. Dr. Michael Welch and Ms. Carla Mathias have attached out BAT reagent to the protein albumin and now to antibodies. PET animal studies with this agent have been very promising.

Using specific and biologically active, radiolabeled MoAb, such as Lym-1, L-6, and Ch L-6 the influence of factors, such as amount of administered MoAb; amount and schedule for administered radionuclide; radiation dose rate; alterations to tumor delivery by use of internalizing Moabs ;variations in the charicteristics of the radionuclide,chelate,linkage, and site-specific attachments for radionuclides will continue to be studied. Methods to be used include: those developed in the last 3-5 years in this DOE program; quantitative imaging that provides absolute amounts (and concentrations) of MoAb in tumor and organs for pharmacokinetics and radiation dosimetry in patients; tomographic imaging estimates of tumor volume; and in vitro tests for in vivo cytotoxicity. Statistical and protocol designs are used which provide the most information from a minimum number of patients.

Strengths of this ongoing program include: an interactive, interdisciplinary investigative team, investigators who bridge the interface between basic and clinical sciences; use of "state-of-the-art" methods in chemistry, immunochemistry, molecular biology, radiopharmacy, imaging and computer software already established and in many instances developed by the group under this DOE program; and existence of established resources and specialized laboratory investigators.

RADIOIMMUNOTHERAPY: DEVELOPMENT OF AN EFFECTIVE APPROACH

PROGRAM GOAL:

TO ANSWER THE FUNDAMENTAL SCIENTIFIC QUESTIONS FOR THE DEVELOPMENT OF AN EFFECTIVE APPROACH FOR DELIVERING RADIATION THERAPY TO CANCER ON ANTIBODY-BASED RADIOPHARMACEUTICALS.

DURING THE CURRENT GRANT PERIOD, OCTOBER 1990-91, THE FOLLOWING DEVELOPMENTS WERE HIGHLIGHTS OF OUR PROGRAM:

* DEVELOPMENT OF $^{111}In/^{90}Y$ BAD (DOTA) LYM-1 AS A POTENTIAL THERAPEUTIC RADIOPHARMACEUTICAL SYSTEM
* DOCUMENTATION OF FAVORABLE PHARMACOKINETICS OF ^{111}In BAD (DOTA) LYM-1 IN PATIENTS
* GENETIC ENGINEERING OF SELECTED PORTIONS OF LYM-1 FOR NEW RADIOPHARMACEUTICALS WITH SELECTED MOLECULAR STRUCTURE
* DOCUMENTED DURABLE COMPLETE REMISSIONS IN LYMPHOMA PATIENTS RECEIVING HIGHER RADIATION DOSE RATE FROM INJECTIONS OF 80-100 mCi I-131 LYM-1 PER METER SQUARE BODY SURFACE AREA
* DEVELOPMENT OF ^{67}Cu BAT (TETA) LYM-1 AS A POTENTIAL THERAPEUTIC RADIOPHARMA-CEUTICAL, WITH PATIENT PHARMACOKINETIC STUDIES AND LOW DOSE THERAPEUTIC RESPONSES IN PATIENTS WITH LYMPHOMA
* FURTHER DEVELOPMENT AND APPLICATION OF QUANTITATIVE RADIONUCLIDE IMAGING TECHNIQUES AND COMPUTER SOFTWARE DEVELOPMENT TO PROVIDE FOR THERAPY PLANNING AND DOSIMETRY CALCULATIONS FROM IMAGING PHARMACOKINETICS
* QUANTITATIVE IMAGING, PHARMACOKINETICS, AND DOSIMETRY LEADING TO RADIOIMMUNOTHERAPY IN BREAST CANCER

DURING THIS 12 MONTH PERIOD, 13 PAPERS HAVE BEEN PUBLISHED OR ARE IN PRESS. TWENTY-FOUR ABSTRACTS HAVE BEEN PUBLISHED; AND 10 NATIONAL AND 5 INTERNATIONAL INVITED LECTURES HAVE BEEN GIVEN.

DOE SUPPORTED PUBLICATIONS THIS YEAR (1990-1991)

1990 Meares, C.F., M.K. Moi, H. Diril, D.L. Kukis, M.J. McCall, S.V. Deshpande, S.J. DeNardo, D. Snook, A.A. Epenetos. Macrocyclic chelates of radiometals for diagnosis and therapy. International Journal of Cancer 62:21-26.

1990 DeNardo, S.J., S.V. Deshpande, M.K. Moi, G.P. Adams, M.J. McCall, G.L. DeNardo, C.F. Meares. Today and tomorrow: radiochemistry for radioimmunotherapy of breast cancer. Frontiers of Radiation Therapy and Oncology 24:142-150.

1990 McCall, M.J., H. Diril, C.F. Meares. Simplified method for conjugating macrocyclic bifunctional chelating agents to antibodies via 2-iminothiolane. Bioconjugate Chemistry 1:3, 22-226.

1991 DeNardo, G.L., S.J. DeNardo, D. Kukis, H. Diril, C. Suey, C. Meares. Strategies for enhancement of radioimmunotherapy. Nuclear Medicine and Biology 18:633-640.

1991 DeNardo, S.J., L.F. O'Grady, D.J. Macey, L.A. Kroger, G.L. DeNardo, K.R. Lamborn, N.B. Levy, S.L. Mills, I. Hellstrom, K.E. Hellstrom. Quantitative imaging of mouse L-6 monoclonal antibody in breast cancer patients to develop a therapuetic strategy. Nuclear Medicine and Biology 18:621-631.

1991 DeNardo, S.J., K.A. Warhoe, L.F. O'Grady, G.L. DeNardo, I. Hellstrom, K.E. Hellstrom, S.L. Mills. Radioimmunotherapy with I-131 chimeric L6 in advanced breast cancer. In: Breast Epithelial Antigens, R.L. Ceriani (eds.), Plenum Press, New York, pp. 227-232.

1991 Adams, G.P., S.J. DeNardo, A. Amin, L.A. Kroger, G.L. DeNardo, I. Hellstrom, K.E. Hellstrom. Comparison of the pharmacokinetics in mice and the biological activity of murine L6 and human-mouse chimeric Ch-L6 antibody. Antibody, Immunoconjugates, and Radiopharmaceutic als (In Press).

1991 Gobuty, A, G.L. DeNardo, S.J. DeNardo. Lym-1 radioimmunotherapy: a case history of how we do it. Antibodies, Immunoconjugates and Radiopharmaceuticals (In Press).

1991 DeNardo, G.L., S.J. DeNardo, C.F. Meares, D. Kukis, H. Diril, M.J. McCall, G.P. Adams, L.F. Mausner, D.C. Moody, S.V. Deshpande. Pharmacokinetics of Copper-67 conjugated Lym-1, a potential therapeutic radioimmunoconjugate, in mice and in patients with lymphoma. Antibodies, Immunoconjugates and Radiopharmaceuticals (In Press).

1991 DeNardo, S.J., K.A. Warhoe, L.F. O'Grady, I. Hellstrom, K.E. Hellstrom, S.L. Mills, D.J. Macey, J.E. Goodnight, G.L. DeNardo. Radioimmunotherapy for breast cancer: treatment of a patient with I-131 L6 chimeric monoclonal antibody. The International Journal of Biological Markers (In Press).

1991 DeNardo, S.J., G.L. Denardo, L.F. O'Grady, K.A. Warhoe, D.J. Macey, L.A. Krogrer, K.E. Hellstrom, I. Hellstrom. Radioimmunotherapy Studies in Breast Cancer. Proceedings of Radiation Research: A Twentieth-Century Perspective, Vol. 2, Toronto, Canada (In Press).

1991 DeNardo, G.L., S.J. DeNardo, N. Levy. Treatment of B cell malignancies with ^{131}I-Lym-1 and mechanisms for improvement. Epenetos (eds), Chapman & Hall Publishing (In Press).

1991 Warhoe, K.A., S.J. DeNardo, H.B. Wolkov, E.C. Doggett, L.A. Kroger, K.R. Lamborn, G.L. DeNardo. Evidence for external beam irradiation enhancement of radiolabeled monoclonal antibody uptake in breast cancer. Antibodies, Immunoconjugates and Radiopharmaceuticals (In Press).

1991 O'Grady, L.F., S.J. DeNardo, G.L.DeNardo. Radioimmunotherapy of lymphoproliferative disease: toxicity studies. Journal of Clinical Oncology (Submitted).

1991 Macey, D. J., S. J. DeNardo, G.L. DeNardo. Estimation of radiation absorbed doses to the red marrow in radioimmunotherapy. American Journal of Physiology Imaging (Submitted).

1991 Macey, D.J., G.L. DeNardo, S.J. DeNardo. Planar Gamma Camera Quantitation of I-123, Tc-99m or In-111 in the Liver and Spleen of an Abdominal Phantom. Journal Physiol. Imaging (Submitted).

1991 DeNardo, G.L., J.P. Lewis, S.J. DeNardo, L.F. O'Grady. Impact of lym-1 Radioimmunoconjugate on refractory chronic lymphocytic leukemia. Cancer (Submitted).

1991 Mills, S.L., S.J. DeNardo, G.L. DeNardo. Radiopharmaceutical preparation of a monoclonal antibody, Lym-1 for therapy of B-cell lymphoma with I-131 a four year review. Journal of Nuclear Medicine (Submitted).

1991 Mathias, C.J., M.J. Welch, M.A. Green, H. Diril, C.F. Meares, R.J. Gropler, S.R. Bergmann. In vivo comparison of copper blood pool agents: potential radiopharmaceuticals for use with copper-62. The Journal of Nuclear Medicine (Submitted).

OBJECTIVE

TO ANSWER THE FUNDAMENTAL SCIENTIFIC QUESTIONS FOR THE DEVELOPMENT OF AN EFFECTIVE APPROACH FOR DELIVERING RADIATION THERAPY TO CANCER ON ANTIBODY-BASED RADIOPHARMACEUTICALS.

RESEARCH PLAN

I. To Develop Radioimmunopharmaceuticals for Cancer Therapy

A. To determine radionuclide choices appropriate for therapy to solid tumors, to infiltrating bone marrow tumor, and to leukemic or intracavitary single cell disease.

B. To develop and test antibody radiopharmaceuticals from new radiochelates designed to completely control the chosen radiometals in vivo.

1. To develop new chelates for Cu-67 with improved metabolic properties, for better biodistribution and imaging results in human patients.
2. To develop a macrocycle/linker family that will completely control both In-111 and Y-90.
3. To test the antibody-macrocycle conjugates for their ability to hold desirable therapeutic and positron emitting radiometals under physiological conditions and during catabolism in vivo by pharmacokinetic studies in patients.
4. To test the feasibility of effective therapy with these agents when indicated (i.e. ^{67}Cu-BAT(TETA)-Lym-1, ^{111}In/^{90}Y-BAD(DOTA)-Lym-1, ^{111}In/^{90}Y-BAD(DOTA)-ChL-6.

C. To seek the most effective chelate-antibody linkage(s) for rapid clearance of the radiochelate from liver and other normal organs, while maintaining retention of the antibody-radiochelate conjugate on the tumor cell surface.

D. To build more effective tumor targeting molecules by recombinant technology using as the initial building block of the molecular structure of the antigen binding region from chosen MoAb clones.

II. To Develop Therapy Planning Based on Quantitative Imaging

A. To utilize quantitative imaging to evaluate selected developmental radiopharmaceuticals.

1. To obtain quantitative pharmacokinetics and tumor uptake information in a mode which allows statistical evaluation of the validity of the information about a radiopharmaceutical from a few patient studies.

B. To utilize planar quantitative imaging techniques that we have developed to obtain radiopharmacokinetic data on serial therapy doses in patients.

C. To utilize this information to calculate the radiation dose to the patients, their normal organs and tumors for each therapy dose.

D. To develop S.P.E.C.T. quantitative methods to determine more accurate normal organ uptake and tumor uptake, particularly in tumors deep in the body.

E. To correlate the projected therapy dosimetry with that actually observed/correlate with information from autoradiography of biopsies, and in vivo quantitation of the radioactivity.

F. To determine the most effective manner to utilize this approach to plan a treatment course and to predict responses.

III. To Develop and Implement Methods to Increase Tumor Delivery and Therapeutic Index of the Radioimmunopharmaceutical in Cancer Patients.

A. To use MoAbs and chimeric MoAb chosen and/or developed containing the effector cell signals to create inflammatory response at tumor sites, causing increased vascular permeability.

B. To develop immunoconjugates by recombinant technology reproducing the selected molecular structure which retains immunoreactivity, carry the appropriate chelate for radiometal, and have effective size/charge characteristics for enhanced tumor delivery and hepatocyte metabolism.

C. To develop radioimmunoconjugates with internalizing MoAbs and compare their radiobiologic effect in vitro and in vivo to that of membrane bound radioimmunopharmaceuticals

D. To develop and study human pharmacokinetics and therapy feasibility of Cu-67 and Y-90 radioimmunotherapeutic pharmaceuticals for lymphoma and adenocarcinoma with tumor cell membrane targeting MoAb radiopharmaceuticals.

RESEARCH ACCOMPLISHMENTS (PROGRESS)

A. DEVELOPMENT OF DOSIMETRIC APPROACHES TO TREATMENT PLANNING FOR RADIOIMMUNOTHERAPY

1. Major Accomplishments

The objective of quantitative imaging is to provide pharmacokinetic information for patients that is analogous to that provided by biodistribution studies in mice. Radionuclide images depict the distribution of labeled antibodies in-vivo; thus the amount of radionuclide in a specific organ or site can be estimated by relating the counts detected in a defined region of interest to the total radionuclide content. This pharmacokinetic information can be used to obtain definitive answers to basic questions of importance for optimizing radioimmunoimaging and radioimmunotherapy and, in addition, can provide a data base from which to calculate the distribution of radiation absorbed doses. The projects supported by this program routinely employ quantitative imaging in evaluating therapies.

Considerable work has been done on the computer programs used. A comprehensive software system has been developed to provide pharmacokinetic data and radiation dosimetry for any portion of a patient from sequential planar images of patients who received radiolabeled antibody. This software, in concert with our quantitative imaging methods, provides a major step in our ultimate goal to develop a comprehensive treatment planning approach which allows us to evaluate individual patients relative to the suitability of radioimmunotherapy, and to compare therapeutic efficacy and toxicity with estimated radiation absorbed doses. The program provides calculated radiation absorbed doses for: the whole body, the red marrow and tumors/organs that demonstrate detectable uptake of a radiolabeled monoclonal antibody (MoAb) in sequential gamma camera images. Various options in this computer program provide organ and tumor volumes from SPECT images, attenuation correction factors for various sites from a whole body transmission image, and allow the user to visualize and stack images in various time sequences that aid clinical interpretation.

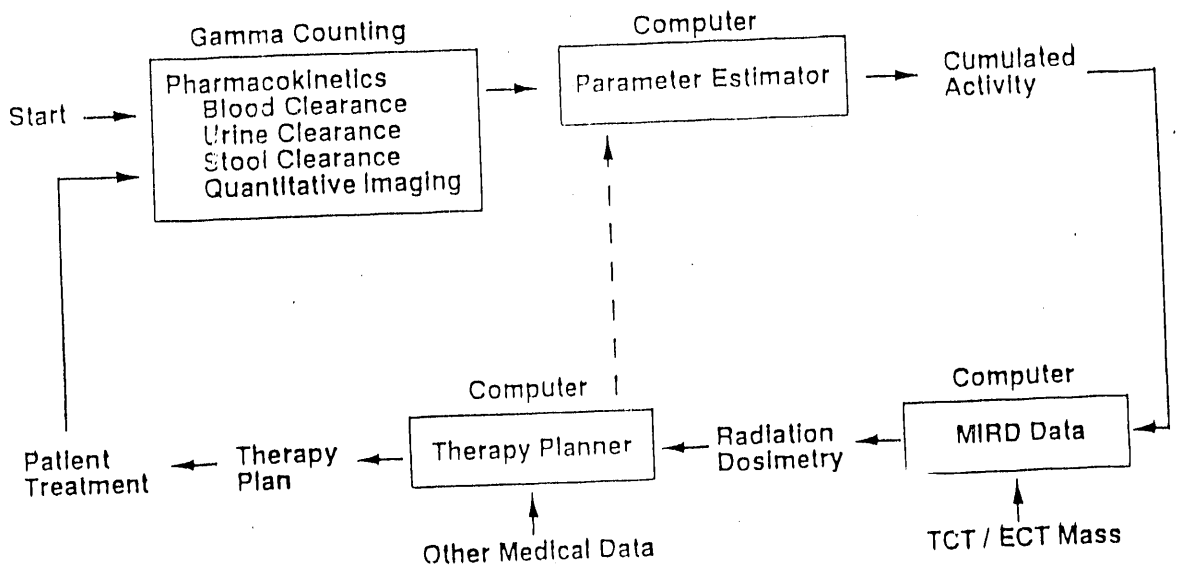

Figure 1. Treatment planning system. A parameter estimator is applied to patient data to obtain cumulated activity. These estimates are used as inputs to a therapy planner along with MIRD and mass data to obtain radiation dosimetry. A therapy planner incorporates other medical data to reach a therapy plan for the patient that can incorporate the radiopharmaceutical studied, the same MoAb with a different radionuclide, or a fragment of the same MoAb (where the different behaviors are available). The process is iterated, if necessary, to complete the therapy regimen.

2. Organizational Structure

Dr. G. DeNardo and the medical physicist direct the quantitative imaging and dosimetry section and are responsible for the overall management of the microVAX II quantitative imaging data base. Dr. Macey and Dr. Groch provide support in the area of imaging and dosimetry software development.

3. Specific Illustrations

Studies of Abdominal Phantom

Transmission and emission images of a phantom (Alderson phantom) which was designed to simulate the abdomen of a patient were obtained in a manner analogous to that used for quantitative imaging of patients in an effort to assess the accuracy of the method and influence of background radioactivity. The simulated liver and spleen were filled with water containing an accurately assayed amount of radionuclide sufficient to provide a concentration of radioactivity comparable to that observed in patients who had received radiolabeled antibody. Water containing no radioactivity, or a concentration of radioactivity equal to 7% or 14% of that placed in the liver and spleen was put in the concavity of the trunk of the phantom that surrounded the liver and spleen. In the absence of background radionuclide in the abdominal phantom and in the absence of background subtraction, the radionuclidic content of the liver or spleen was accurately quantitated by the described methods, including the use of a first order attenuation correction factor determined by transmission imaging (Figure 2). However, radionuclidic content of the liver or spleen was less accurately determined in the presence of radionuclide in the surrounding phantom regardless of whether general phantom background was subtracted or not. Radionuclidic content was over-estimated when background radionuclide was not subtracted. The errors were greater for the spleen than for the liver and greater when larger amounts of radionuclide were placed in the abdominal phantom. Similar studies for tumors ranging from 2 to 5 cm in diameter indicated that they can be accurately quantitated as well.

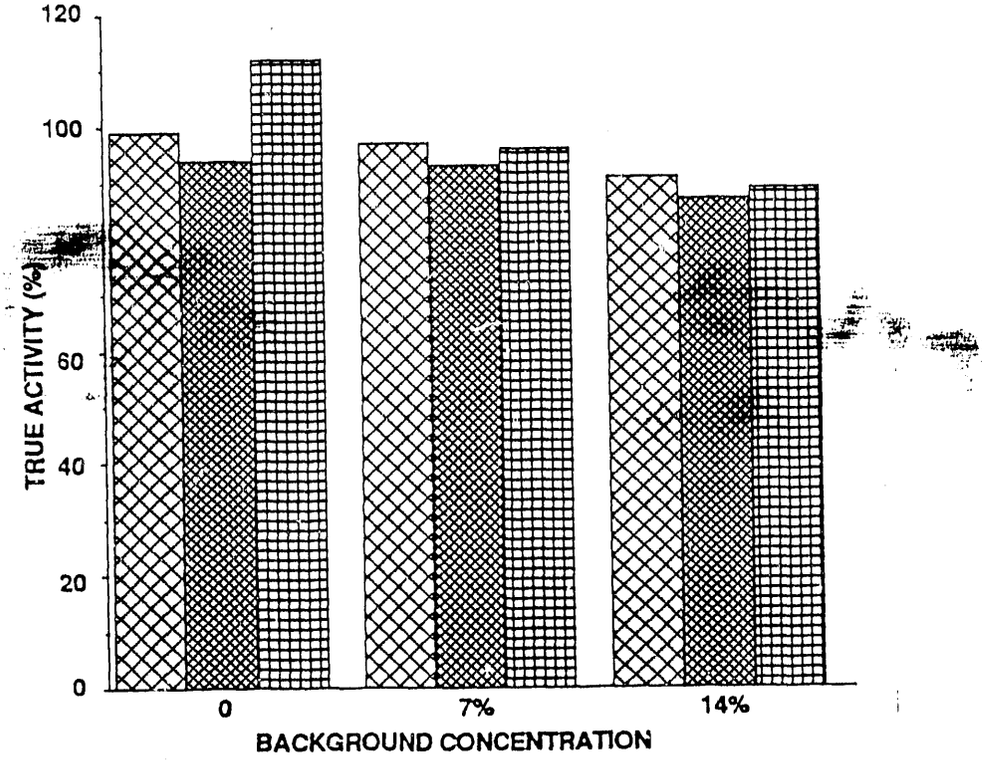

Figure 2. Results of quantitation of I-123, Tc-99m and In-111 in simulated liver of an abdominal phantom in the absence of and presence of Tc-99m in the surrounding phantom using the geometric mean method and attenuation correction factors for the liver determined by transmission imaging. Quantitations were accurate when background was subtracted.

B. TETA AND DOTA LYM-1 DEVELOPMENT AND $^{67}Cu/^{90}Y$ PHARMACOLOGY

Studies in Mice

The TETA macrocycle and the DOTA macrocycle tightly bind ^{67}Cu and ^{88}Y, respectively, in physiologic milieu and can be conjugated to Lym-1 with preservation of immunoreactivity. Indium and yttrium-BAD-Lym-1 (chelated by DOTA) behave the same in mice and are tightly bound so that indium does not escape to the reticuloendothelial system and yttrium to the skeleton as has been the case with other chelates. This provides an exciting system for pharmacologic and subsequent therapeutic trials in patients. Similarly, biodistribution studies of ^{67}Cu-BAT(TETA)-Lym-1 in mice have confirmed that it is tightly bound and has great promise as an imaging and therapeutic radionuclide for patients. Pharmacologic biodistribution studies of ^{67}Cu and ^{90}Y Lym-1 have been completed in athymic mice bearing human Raji lymphoma. When injected into lymphoma-bearing mice, the tumor accumulation and retention of these constructs is greater than that of iodinated Lym-1. Furthermore, there is no accumulation in the bone marrow in contrast to the results obtained by other investigators for yttrium labeled antibodies conjugated by other chelates. If proven in patients, this avoids a significant source of marrow radiation that led to termination of two clinical trials in which other yttrium-chelated antibodies were utilized.

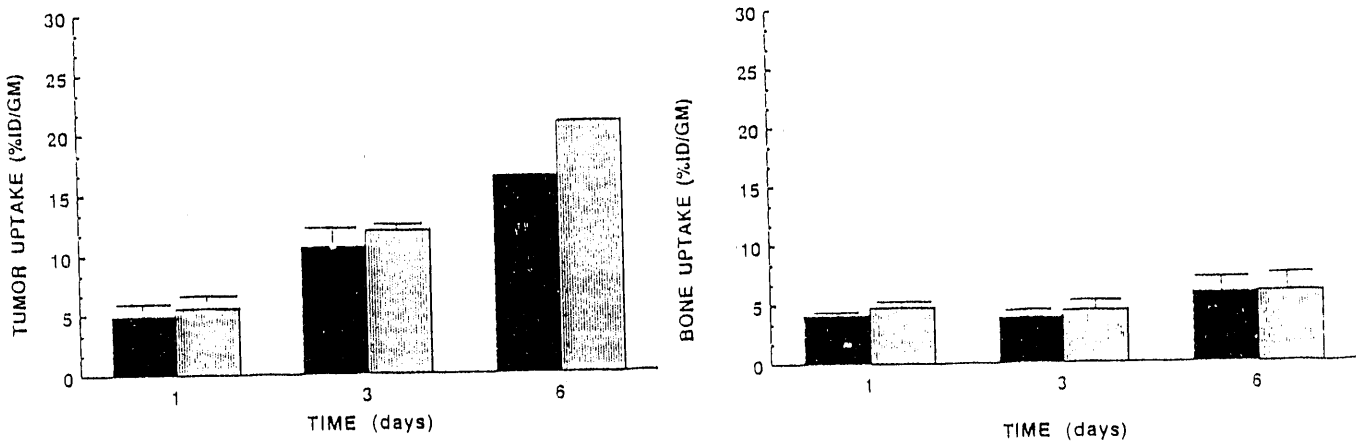

Figure 3. A. Correlation of concentrations of ^{111}In (■) and ^{88}Y (▨)-2IT-BAD Lym-1 in Raji human lymphoma implanted in nude mice (N ≥3). B. Correlation of concentrations of ^{111}In (■) and ^{88}Y (▨)-2IT-BAD Lym-1 in bone (without marrow) from nude mice (N≥3).

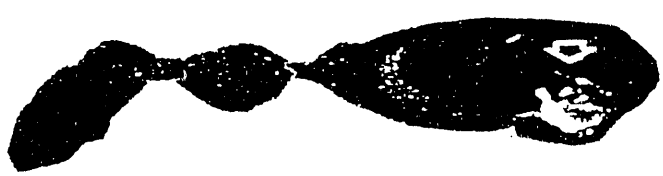

Figure 4. Autoradiography of a nude mouse 5 days after injection with ^{90}Y-BAD(DOTA)-Lym-1. The arrow indicates a Raji tumor with good uptake. The other area seen is the liver.

Studies in Patients

General

The objective of quantitative imaging is to provide pharmacokinetic information for patients that is analogous to that provided by biodistribution studies in mice. Radionuclide images depict the distribution of labeled antibodies in-vivo; thus the amount of radionuclide in a specific organ or site can be estimated by relating the counts detected in a defined region of interest to the total radionuclide content. This pharmacokinetic information can be used to obtain definitive and relevant answers to basic questions of importance for optimizing radioimmunoimaging and radioimmunotherapy and, in addition, can provide a data base from which to calculate the distribution of radiation absorbed doses. The clinical projects supported by this program routinely employ quantitative imaging in evaluating therapies. A correlation between the concentration of radionuclide observed by counting biopsy samples and that observed by quantitative imaging was found (Figure 5).

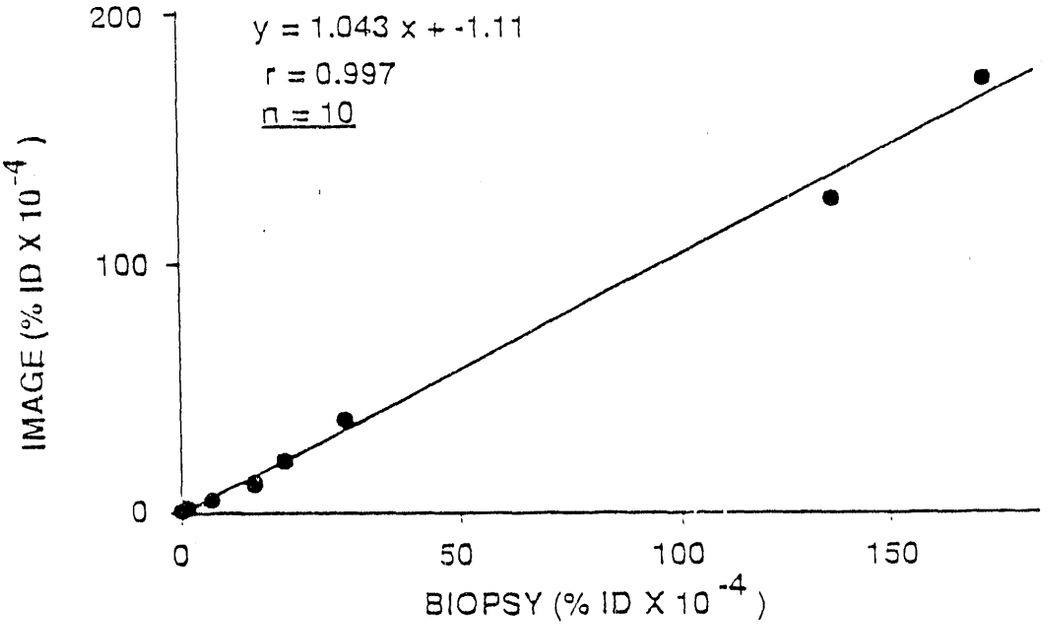

Figure 5. Correlation of tumor concentration of I-131 Lym-1 determined by counting biopsy sample and imaging patient.

Studies have also been initiated to identify possible sources of error in dose calculations. The influence of remaining body activity on the calculated radiation absorbed doses delivered to various organs/sites in the body has been investigated for patients receiving diagnostic and therapy doses of I-131 labeled Lym-1 considering the liver as both the target and the source. Good agreement was found using the corrected cumulated activity and the corrected 'S' factor methods. Doses are overestimated by up to 20% for the liver using the straightforward MIRD approach. This correction factor is small for typical tumor sites of less than 100 ml with uptakes of less than 1% of the administered dose. The magnitude of this correction factor for organs and uptake sites at various distances from high uptake organs/sites in the body merits further consideration. The remaining body activity correction factor can be elegantly calculated for any site in the body from a whole body image. The validity of the remaining whole body activity approach can be examined and refined for a specific target organ/site in the body.

Transmission and emission images of patients who had received intravenous antibodies labeled with In-111, I-123, Cu-67 or I-131 were obtained and quantitations performed by previously described methods.

Using the techniques described, an observer became capable of obtaining reproducible quantitative results after modest experience. Greater effort was required for two observers to obtain results comparable to each other. The major impediment to the achievement of reproducible results was related to the choice of the region for background radioactivity. There was a propensity in all instances for background estimates to be excessive, so that a region of least body background was selected.

^{67}Copper BAT(TETA) Lym-1 Imaging Pharmacology Studies.

We have particularly focused upon radionuclide and radiochemical improvements because of our recognition that ^{131}I was not an ideal radionuclide for radioimmunotherapy and because of the unique strengths of our group in radiochemistry. The requirements for an ideal therapeutic radionuclide are more demanding than those for an imaging radionuclide. The choices of radionuclide and conjugation techniques can substantially affect the radiopharmaceutical stability and in vivo pharmacokinetics thereby influencing the radiation dose distribution and the efficacy of treatment. While ^{131}I is a practical radionuclide, it is not an ideal radionuclide for radioimmunotherapy because of "dehalogenation" and substantial imaging and radiation safety problems secondary to multiple energetic photons. A variety of metals have been advocated for radioimmunotherapy because of superior physical characteristics and observations that their retention in tumors was longer than that of the corresponding radioiodinated antibody leading to an increased radiation absorbed dose to the tumor. For ten years we have advocated and explored the use of ^{67}Cu as a therapeutic radionuclide for radioimmunotherapy.

TABLE 1. Properties of Copper-67

Half life: 62 hours
Decay mode: beta minus
Beta energy/abundance (Emax, keV): 577(20%), 486(35%), 395(45%)
Gamma energy/abundance (keV): 92(24%), 184(47%)
Decay product: ^{67}Zn

Collaborations with Drs. Mausner and Srivastava of the Brookhaven National Laboratory and others at the Los Alamos National Laboratory have led to an acceptably reliable supply of chemically and radionuclidically pure ^{67}Cu. Meares has developed a new macrocycle, TETA, specifically designed to chelate ^{67}Cu (Figure 6). This macrocycle, a derivative of polyazamacrocycles (bearing a side chain for antibody attachment) binds Cu with remarkable chemical inertness.

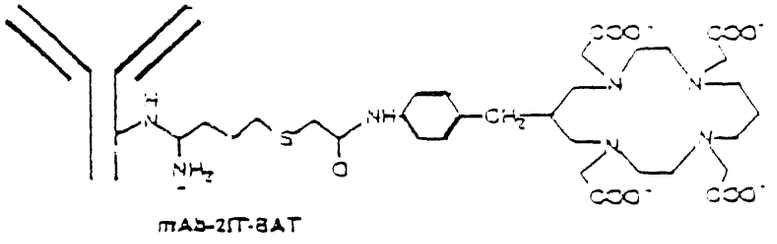

Figure 6. Structural formula of ^{67}Cu-BAT(TETA)-Lym-1.

The radiochemistry required to use TETA and DOTA to conjugate ^{67}Cu or ^{90}Y, respectively, to Lym-1 has been completed as have the procedures necessary to prepare sterile and pyrogen free radiopharmaceuticals. All preclinical studies including mouse studies with ^{67}Cu-BAT(TETA)-Lym-1 or ^{90}Y-BAD(DOTA)-Lym-1 have been completed. Pharmacokinetics in mice implanted with Raji human lymphoma confirmed the superiority of these formulations over earlier ones relative to radiochemical stability and marrow toxicity. INDs for clinical studies for each radiopharmaceutical are in place. Pharmacokinetic studies with ^{67}Cu-BAT(TETA)-Lym-1 have been obtained in eight patients. The pharmacokinetics in these eight patients verified our original anticipation that this would be an exciting therapeutic as well as quantitative imaging radionuclide.

Radiochemical/Radiopharmaceutical Quality. All of the ^{67}Cu-BAT(TETA)-Lym-1 preparations had fewer than three chelates on each antibody molecule when assayed by ^{57}Co (Table 2). Loss of radiolabel from ^{67}Cu-BAT(TETA)-Lym-1 was due to loss of radiometal from the chelate as opposed to loss of the radiochelate from the antibody. This conclusion was chromatographically evident by the observed binding of copper with albumin, the serum protein for which copper is known to have an association in vivo. The rate of transcomplexation of ^{67}Cu from ^{67}Cu-BAT(TETA)-Lym-1 was found to be 0.3 percent per day. In contrast, over 95% of ^{67}Cu has been found to transcomplex from ^{67}Cu-CITC-Lym-1 or ^{67}Cu-DTPA-Lym-1.

Table 2. Characteristics of Radiochemicals/Radiopharmaceuticals

	^{67}Cu-BAT(TETA)-Lym-1 Chelates/MoAb	Radiochemicals/Radiopharmaceuticals Yield (%)	Purity (%)	Immunoreactivity (%)
Preclinical	2.7	≥80	≥90	≥75
Clinical*	0.8-1.3	---	≥90	≥90

* Data reflects 2 chelated Lym-1 lots and 4 radiolabelings; the initial patient preparation was less satisfactory than indicated on this table.

Pharmacokinetics. ^{67}Cu-BAT(TETA)-Lym-1 has proven to be relatively stable in vitro and in vivo in biologic milieus. The pharmacokinetics of ^{67}Cu-BAT(TETA)-Lym-1 in mice and in patients has been the subject of publications attached to this document. The pharmacokinetics of radioiodinated Lym-1 has been extensively explored in nude mice implanted with human lymphoma and in patients under tracer and therapeutic radionuclide conditions. There is no evidence of "dehalogenation" of radioiodinated Lym-1 in the Raji human lymphoma nude mouse model. Uptake and retention of radioiodinated Lym-1 by the Raji lymphoma is good and there is no evidence of active uptake of Lym-1 by normal tissues. The pharmacokinetics of ^{67}Cu-BAT(TETA)-Lym-1 in this nude mouse model were comparable to those of radioiodinated Lym-1. There was good uptake and retention of ^{67}Cu-BAT(TETA)-Lym-1 by the tumor, no evidence of skeletal or bone marrow uptake or of other normal tissue uptake. While liver uptake and retention of ^{67}Cu-BAT(TETA)-Lym-1 was nominally greater than that of radioiodinated Lym-1, the difference was not significant.

Pharmacokinetics of ^{67}Cu-BAT(TETA)-Lym-1 were studied in eight patients using blood, fecal and urinary clearance methods and quantitative imaging. The radiopharmaceutical was less than optimum in one patient whose blood clearance was rapid and a second patient had a slower than usual blood clearance of ^{67}Cu-BAT(TETA)-Lym-1 and of ^{131}I-Lym-1. The blood clearance of ^{67}Cu-BAT(TETA)-Lym-1 was similar to that observed for ^{131}I-Lym-1 for two days after injection but subsequently there was greater flatness of clearance of ^{67}Cu suggesting possibly a small percentage of ^{67}Cu may be recycling as a metabolite into the blood from a tissue, such as the liver.

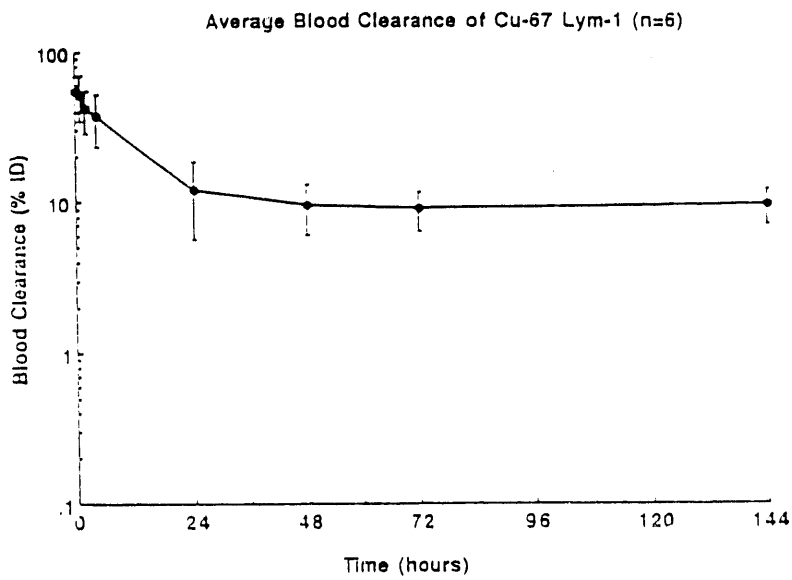

Figure 7. Blood clearance of ^{67}Cu-BAT(TETA)-Lym-1 observed in six patients (mean ± 1 SD). Blood clearances of three of the patients were similar to those for ^{131}I-Lym-1 for 48 hours and then deviated. One patient had slow clearance of ^{67}Cu-BAT(TETA)-Lym-1 corresponding to slow clearance of a sub-sequent dose of ^{131}I-Lym-1 and the first patient had a rapid early clearance because of a suboptimal radiopharmaceutical.

There was almost no ^{67}Cu in the initial two hour urine specimens from the patients indicating an absence of free ^{67}Cu-BAT(TETA), and subsequent urinary excretion of ^{67}Cu was less than that observed for patients that had received ^{131}I-Lym-1. Whole body counting and urinary excretion indicated that the clearance of ^{67}Cu from the patients was slower than that of ^{131}I. Excretion of ^{67}Cu into the feces was small in amount and only slightly greater than that of ^{131}I. The efficiencies of our scintillation cameras were 5-6 times greater for ^{67}Cu than for ^{131}I despite the lesser abundance of ^{67}Cu photons. This relates to the fact that the photons of ^{67}Cu are ^{99m}Tc-like in energy and more efficient for a scintillation camera than the more energetic photons of ^{131}I. For the same amount of radioactivity and number of counts, superb images were obtained six times faster after injection of ^{67}Cu-BAT(TETA)-Lym-1 than after injection of ^{131}I Lym-1. The quality and resolution of the ^{67}Cu images were much superior to those obtained with ^{131}I.

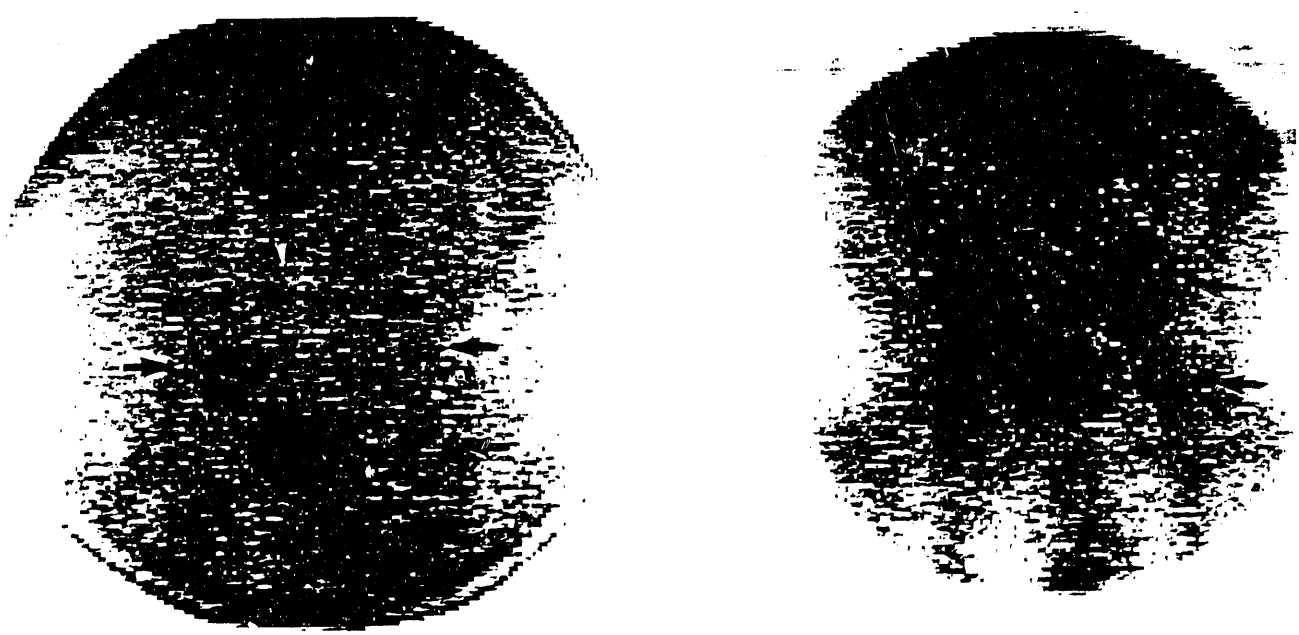

Figure 8. Anterior images of the abdomen and pelvis of a patient with lymphoma obtained 24 hours after injection of 10 mCi of ^{131}I-Lym-1 (left) or ^{67}Cu-BAT(TETA)-Lym-1 (right). Iliofemoral tumors are better visualized with ^{67}Cu-BAT(TETA)-Lym-1 despite increasing the intensity of the computer generated ^{131}I-Lym-1 image 3 times higher than that for the ^{67}Cu-BAT(TETA)-Lym-1 image. This was necessary because of greater clearance of ^{131}I-Lym-1 from the tumors.

There was no evidence of active uptake of ^{67}Cu by any normal tissue. Specifically, there was no uptake of ^{67}Cu by the stomach, thyroid or salivary glands as is the case for ^{131}I. However, retention of ^{67}Cu by the liver was longer than that of ^{131}I leading to a modestly greater radiation absorbed dose.

Table 3. Radiation Dosimetry

	Radiation Dose (rads/mCi)
Whole Body	0.3-0.6
Liver	1.6-5.2
Spleen*	3.7-9.1
Kidney	0.5-1.5
Marrow**	0.2-0.7
Tumor***	4.7-20.6
Lung	0.6-1.6

*diseased
**from blood and body
***1.4-5.4 X greater than ^{131}I Lym-1

Importantly, there was no evidence for skeletal or bone marrow uptake of ^{67}Cu in the absence of lymphomatous disease in common with ^{131}I. Radiation absorbed dose to the bone marrow of the patients from blood and whole body contributions was less than that from ^{131}I because of the lesser abundance of photons and shorter physical half-life. Lymphomatous tumor uptake of ^{67}Cu-BAT(TETA)-Lym-1 was as great as that of ^{131}I Lym-1 in all instances and the radiation absorbed dose to the tumors was 1.4-5.4 times greater for ^{67}Cu than for ^{131}I because the ^{67}Cu was retained in the tumors much longer than was ^{131}I. This was particularly dramatic in some patients. Three patients that received 5-10 mCi of ^{67}Cu-BAT(TETA)-Lym-1 had significant decrease in the size of their tumors after administration of the antibody.

Figure 9. Tumor uptake in left inguinal nodes was observed as early as 4 hours (left) and remained constant from 24 hours (right) through 96 hours. This patient's tumor decreased in size during the period of observation. Images of patients after injection of ^{67}Cu-BAT(TETA)-Lym-1 were of good quality and resolution.

No change in tumor size was observed in the other five patients, but the amounts of administered ^{67}Cu were intended for pharmacokinetic rather than therapeutic purposes. None of the patients developed an antiglobulin response (HAMA) against the Lym-1 when tested repeatedly for at least two months following injection.

In summary, the pharmacokinetics and radiation dosimetry of ^{67}Cu-BAT(TETA)-Lym-1 in patients seems highly favorable when compared to that of ^{131}I-Lym-1. The tumor to biologically critical organ (bone marrow) therapeutic ratio is distinctly more favorable for ^{67}Cu-BAT(TETA)-Lym-1 than that of ^{131}I Lym-1.

DOTA Lym-1 Development and In-111/Y-90 Lym-1 Imaging Pharmacology Studies.

Yttruim-90 is a promising radiometal for therapy of cancer due to its high-energy beta emission useful for therapy of solid tumors and its physical half-life of 2.67 days. It can be produced easily by a $^{90}Sr/^{90}Y$ generator. A macrocylic bifunctional chelating agent based on 1,4,7,10-tetraazacyclododecane-N,N',N",N'"-tetraaceetic acid (DOTA) forms a stable yttrium complex. It was converted to p-bromoacetamidobenzyl-DOTA (BAD), and conjugated to Lym-1 via 2-iminothiolane. Stability studies of ^{88}Y-Lym-1-2IT-BAD in human serum in vitro showed no measurable loss of yttrium from the ligand over a 25 day period. The improved method of conjugation to remove high molecular weight species has been worked out and is reported on by McCall (1990). We have manufactured a large batch of the conjugate (Lym-1-2IT-BAD) for human use under FDA guidelines.

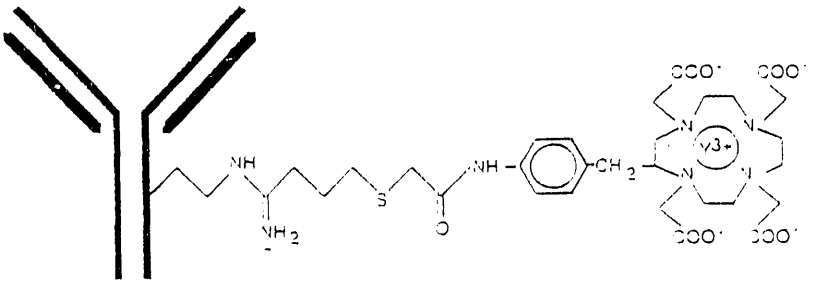

Figure 10. Structural formula of ^{111}In-BAD(DOTA)-Lym-1.

Studies in Patients

Radiochemical/Radiopharmaceutical Quality. All of the ^{111}In-BAD(DOTA)- Lym-1 preparations had 3 chelates on each antibody molecule when assayed by ^{57}Co. By HPLC, all of the radiolabel was associated with the conjugated Lym-1 (~150,000).

Pharmacokinetics. ^{111}In-BAD(DOTA)-Lym-1 and ^{90}Y-BAD(DOTA)-Lym-1 have proven to be relatively stable in vitro in biologic milleus. The pharmacokinetics of ^{111}In-BAD(DOTA)-Lym-1 and ^{90}Y-BAD(DOTA)-Lym-1 in mice have been the subject of publications cited in this document (Deshpande 1989, 1990).

Pharmacokinetics of ^{111}In-BAD(DOTA)-Lym-1 has been studied in 4 patients that received 3.1-5.3 mCi using blood and urinary clearance methods and quantitative imaging. In 3 of these patients this study was followed by an ^{131}I-Lym-1 study. Similar blood clearance curves were seen in the patients with ^{131}I-Lym-1 when compared to ^{111}In-BAD(DOTA)-Lym-1 (Figure 11). The ^{111}In-BAD(DOTA)-Lym-1 had a somewhat slower clearance from the body (and liver) and diminished urinary excretion when compared to ^{131}I-Lym-1 (Figure 12). However, corrected for decay 50% is excreted by Day 6. Therapeutic ratio (T/NT) can be calculated for ^{90}Y by extrapolation of ^{111}In data (see below). If ^{90}Y-BAD(DOTA)-Lym-1 pharmacokinetics in patients correlates to ^{111}In-BAD(DOTA)-Lym-1, as it has in our animal studies, then this will be a good therapeutic agent. Further improvements in dosimetry are expected with the new linkage we have recently developed. (Reported in Chemistry section)

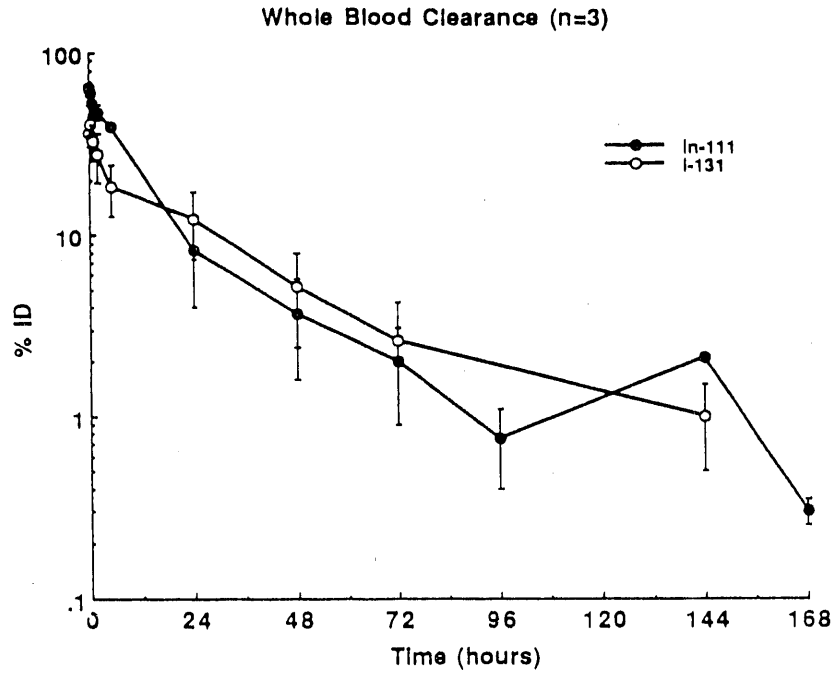

Figure 11. Whole blood clearance of ^{111}In-BAD(DOTA)-Lym-1 was comparable to that of ^{131}I-Lym-1.

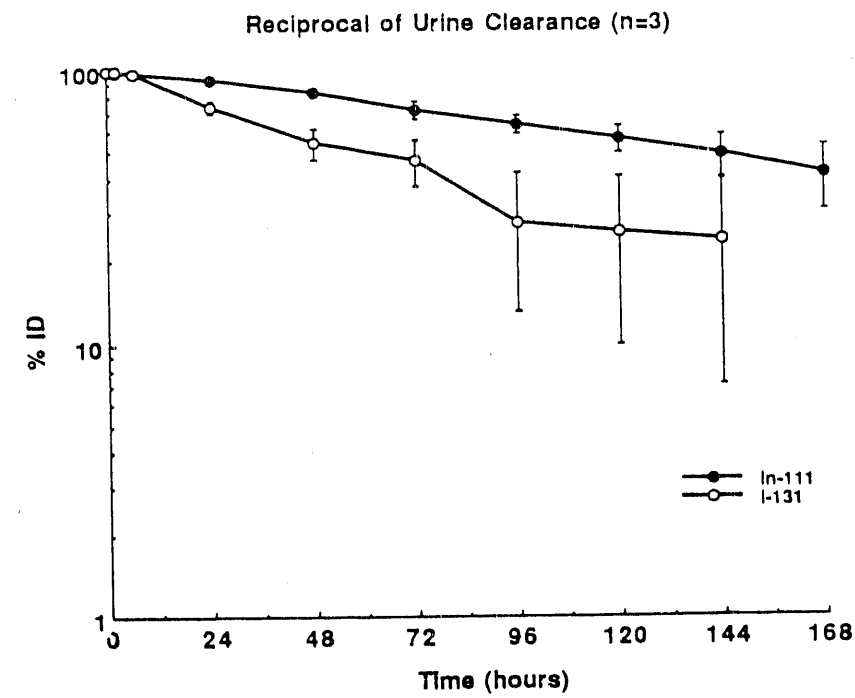

Figure 12. Urinary clearance of ^{111}In-BAD(DOTA)-Lym-1 was diminished when compared to ^{131}I-Lym-1.

Table 4. Radiation Dosimetry

Radiation Dose (rads/mCi)	In-111	Y-90*
Whole Body	0.4	1.7- 2.0
Liver	0.3-2.6	15.5- 21.3
Spleen**	2.2-6.8	27.3- 84.6
Kidney	0.2-0.3	2.7- 3.3
Marrow***	0.03-0.1	2.8- 3.4
Tumor	0.2-7.6	4.6-157.8
Lung	0.2-0.4	3.6- 4.9

*extrapolated from In-111 data
**diseased
***from blood and body

Figure 13. Anterior images of the head (left), chest(middle) and pelvis (right) of a patient with lymphoma obtained 48 hours after injection of 5.2 mCi of In-111-BAD Lym-1. Tumor uptake is easily seen in lymphoma of the skull, soft tissue of the temples, nodes in the neck, mediastinum, axilla, chest, abdomen, pelvis and left inguinal area.

C. MOLECULAR AND STRUCTURAL BIOLOGY/PHARMACEUTICAL DEVELOPMENT

Single-chain antigen-binding proteins produced by recombinant techniques have been suggested to have high potential in cancer therapy. In our opinion they provide the crucial building blocks to initiate designer molecules for antibody based radiopharmaceuticals containing the messages for tumor targeting and vascular permeability as well as radiometal chelates and effective linkage. Our previous sequencing and PCR of the Lym-1 antibody allows us to utilize these methods to create a single-chain version of this antibody. The protein produced can then be modified to improve the properties of our immunoconjugates.

Lym-1 Single-Chain Antigen Binding Protein

The two portions of the SCA protein which encode the variable regions of the Lym-1 antibody were prepared by PCR production of mRNA from Lym-1 cells with several different primers For the light chain, a primer in the constant region was used along with a primer which incorporates a Cfo I site and the terminal amino acids of the ompA signal peptide onto the variable region amine terminus. For the heavy chain, a primer in the signal peptide was used with a primer that incorporates two stop codons and a BamH1 site at the end of the heavy chain variable region. Both of these products were then subcloned into plasmids to enable faithful reproduction of the exact sequences in relatively large quantities. These clones were sequenced to confirm their identities, and then the DNA was grown, isolated and purified. Likewise, the Cloning Site-Operator-Promoter-Signal Peptide fragment was also cloned into a plasmid. This clone was also sequenced and then the DNA was grown, isolated and purified.

The gene was then assembled by successive ligations and gel purifications. The Eco-promoter-ompA fragment was ligated to the light chain fragment at the Cfo I site. The heavy chain fragment was ligated to the Linker at the Ava II site. These were then purified. The Linker/Heavy fragment was then ligated to the Eco-promoter-ompA-Light fragment, purified and ligated into a pUC8 plasmid that had been digested with EcoR1/BamH1 and purified. The recombinants were then selected, and we are currently sequencing them to isolate the proper clones for expression of the SCA protein.

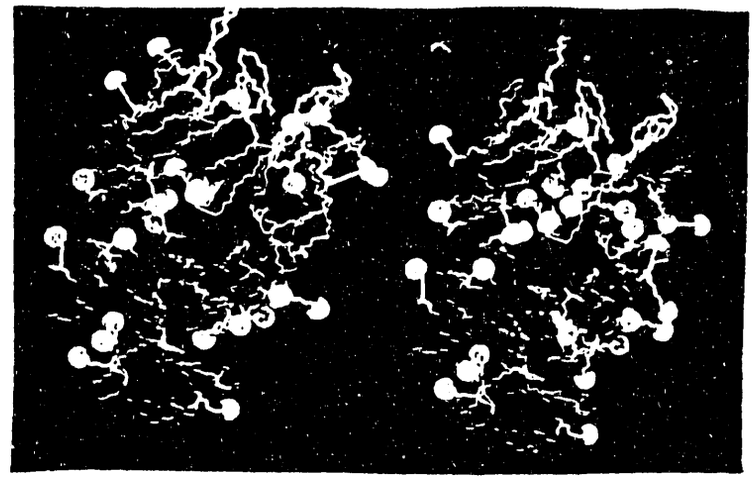

Models of Fab fragments of Lym-1 (left) and Lb (right) mouse IgG2a. Prepared in MIDAS plus on a Silicon Graphics IRS computer, starting with the structure of McPC603 (Sato, Y., Cohen, G.H., Padlan, E.A., and Davies, D.R. (1986) "The phosphocholine binding immunoglobulin Fab McPC603)." J. Mol. Biol. 190:593-604. Lysine side chains yellow; peptide backgone red; hypervariable loops white; N-termini blue.

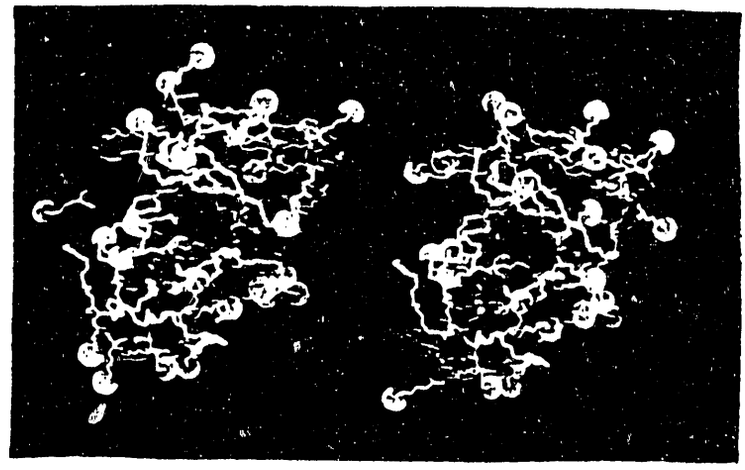

Rotated view of Lym-1 and L6 Fab fragments, with binding sites facing forward. Prepared as figure CHEL-3.

Construction of Lym-1 Single Chain Antigen Binding Protein

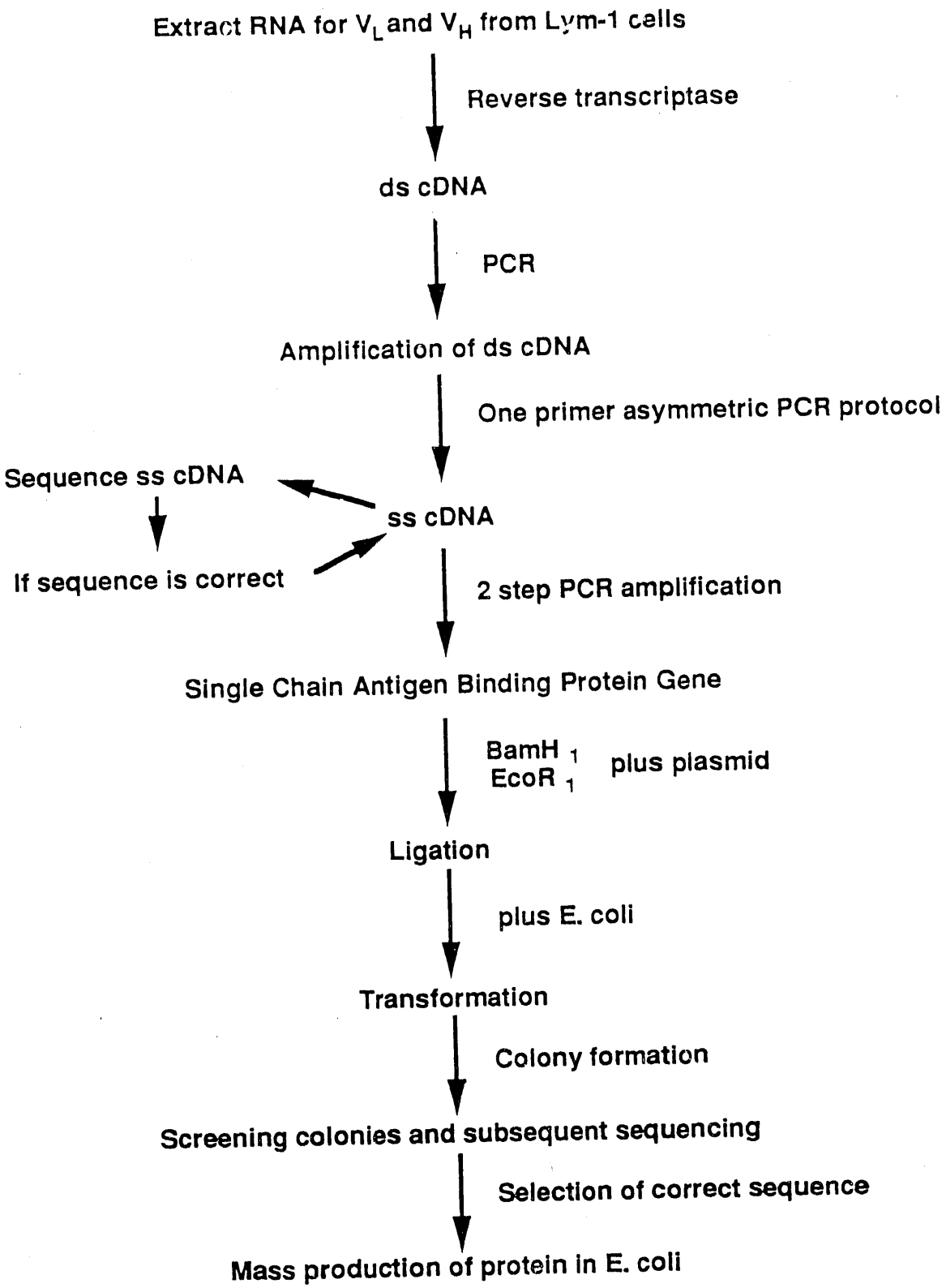

```
CCGGAATTCCGGGATCTCTCTCACCTACCAAACAATGCCCCCCTGCAAAAAATAAATTCATATAAAAAACATACAGATAACCATC
   EcoR1
     OL                                        PR                    +1        SD(cro)
TGCGGTGATAAATTATCTCTGGCGGTGTTGACTATTTTACCTCTGGCGGTGATAATGGTTGCATGTACTAAGGAGGTTGT
                           Hinc2                                          Dde 1
ompA signal                                      -10                                    -1
Met Lys Lys Thr Ala Ile Ala Ile Ala Val Ala Leu Ala Gly Phe Ala Thr Val Ala Gln Ala
ATG AAA AAG ACA GCT ATC GCG ATT GCA GTG GCA CTG GCT GGT TTC GCT ACC GTA GCG CAG GCC
                                                                          Cfo 1
Lym-1 Light Variable                  10                                        20
Asp Ile Gln Met Thr Gln Ser Pro Ala Ser Leu Ser Ala Ser Val Gly Glu Thr Val Thr
GAC ATC CAG ATG ACT CAG TCT CCA GCC TCC CTA TCT GCA TCT GTG GGA GAA ACT GTC ACC
                                      30                                        40
Ile Ile Cys Arg Ala Ser Val Asn Ile Tyr Ser Tyr Leu Ala Trp Tyr Gln Gln Lys Gln
ATC ATA TGT CGA GCA AGT GTG AAT ATT TAC AGT TAT TTA GCA TGG TAT CAG CAG AAA CAG
                                      50                                        60
Gly Lys Ser Pro Gln Leu Leu Val Tyr Asn Ala Lys Ile Leu Ala Glu Gly Val Pro Ser
GGA AAA TCT CCT CAG CTC CTG GTC TAT AAT GCC AAA ATC TTA GCA GAA GGT GTG CCA TCA
                                      70                                        80
Arg Phe Ser Gly Ser Gly Ser Gly Thr Gln Phe Ser Leu Lys Ile Asn Ser Leu Gln Pro
AGG TTC AGT GGC AGT GGA TCA GGC ACA CAG TTT TCT CTG AAG ATC AAC AGC CTG CAG CCT
                                      90                                       100
Glu Asp Phe Gly Ser Tyr Tyr Cys Gln His His Tyr Gly Thr Phe Thr Phe Gly Ser Gly
GAA GAT TTT GGG AGT TAT TAC TGT CAA CAT CAT TAT GGT ACA TTC ACG TTC GGC TCG GGG
                                                                          Ava 1
                                                Linker
Thr Lys Leu Glu Ile Lys Gly Ser Thr Ser Gly Ser Gly Lys Ser Ser Glu Gly Lys Gly
ACA AAG TTG GAA ATA AAA GGT TCT ACC TCT GGT TCT GGT AAA TCT TCT GAA GGT AAA GGT
Lym-1 Heavy Variable                  10                                        20
Gln Val Gln Leu Lys Glu Ser Gly Pro Gly Leu Val Ala Pro Ser Gln Ser Leu Ser Ile
CAG GTG CAG CTC AAG GAG TCA GGA CCT GGC CTG GTG GCG CCC TCA CAG AGC CTG TCC ATC
                              Ava 2
                                      30                                        40
Thr Cys Thr Ile Ser Gly Phe Ser Leu Thr Ser Tyr Gly Val His Trp Val Arg Gln Pro
ACA TGC ACC ATC TCA GGG TTC TCA TTA ACC AGC TAT GGT GTA CAC TGG GTT CGC CAG CCT
                                      50                                        60
Pro Gly Lys Gly Leu Glu Trp Leu Val Val Ile Trp Ser Asp Gly Ser Thr Thr Tyr Asn
CCA GGA AAG GGT CTG GAG TGG CTG GTA GTG ATA TGG AGT GAT GGA AGC ACA ACC TAT AAT
                                      70                                        80
Ser Ala Leu Lys Ser Arg Leu Ser Ile Ser Lys Asp Asn Ser Lys Ser Gln Val Phe Leu
TCA GCT CTC AAA TCC AGA CTG AGC ATC AGC AAG GAC AAC TCC AAG AGC CAA GTT TTC TTA
     82 82A 82B 82C                                  90                        97
Lys Met Asn Ser Leu Gln Thr Asp Asp Thr Ala Ile Tyr Tyr Cys Ala Ser His Tyr Gly
AAA ATG AAC AGT CTC CAA ACT GAT GAC ACA GCC ATA TAC TAC TGT GCC AGT CAC TAC GGT
         100 100A100B                                        110       113
AGT ACC CTT GCC TTT GCT TCC TGG GGC CAC GGG ACT CTG GTC ACT GTC TCT GCA TAA TAA
Ser Thr Leu Ala Phe Ala Ser Trp Gly His Gly Thr Leu Val Thr Val Ser Ala End End

CGCGGATCCGCG
   Bam H1
```

Figure 2. The Lym-1 Single-Chain Antigen-Binding protein gene sequence. The O_L/P_R promoter, *ompA* signal peptide, Lym-1 light and heavy chain variable regions (numbered using the Kabat system), and synthetic linker (underlined) are shown. The restriction sites used to assemble the gene are underlined and labeled.

D. Chelate Chemistry, November 1990 - October 1991

From the beginning, this grant has supported the conception, synthesis, and development of the first macrocyclic bifunctional chelating agent TETA (6-p-nitrobenzyl-1,4,8,11-tetraazatetradecane-N,N',N'',N'''-tetraacetic acid and its derivatives, including Lym-1-2IT-BAT), for use in ^{67}Cu-based radioimmunodiagnosis and therapy. This work has led to the further development of other macrocyclic bifunctional chelating agents for copper and other metals.

Macrocycle Synthesis

The synthesis of 6-(p-Bromoacetamidobenzyl)-1,4,8,11-tetraazacyclotetradecane-N,N',N'',N''',-tetraacetic acid (BAT) is currently carried out following the methods described by Moi (Fig. 1). However, reactions 2 and 4 were modified to improve yields. Reaction 2 was carried out by dissolving 50 g of p-Nitrobenzyldiethylmalonate (**I**) and 27 g of N,N'-Bis(2-aminoethyl)-1,3-propanediamine in 3.5 L of neat ethanol at room temperature and refluxed for 6 days. The product, 3-p-Nitrobenzyl-2,4-dioxo-1,5,8,12-tetraazacyclotetradecane (**II**), was isolated and characterized according to standard procedure. The 2 fold increase in total dilution and the absence of the high dilution reagent addition method modestly increased the yield from 21.4% to 32.8%. Reaction 4 was carried out by dissolving 0.707 g of 6-p-Nitrobenzyl-1,4,8,11-tetraazacyclotetradecane·4 HCl (**III**) in 2.4 mL of H_2O and adjusting the to pH 10 with saturated NaOH. 4 equivalents of bromoacetic acid (0.816 g) were added and again adjusted to pH 10. The reaction mixture was heated to 60 °C and pH 10 was continuously maintained for the duration of the reaction by the addition of 10 M NaOH by a Radiometer pH STAT. After 5 hours, an additional equivalent of Bromoacetic acid was added. Two hours later the reaction was stopped by neutralizing with 6 M HCl. HPLC C-18 purification shows that 6-(p-Nitrobenzyl)-1,4,8,11-tetraazacyclotetradecane-N,N',N'',N''',-tetraacetic acid (**IV**) product yield was marginally improved from 45% to 55%. To date, approximately 0.500 g of **IV** has been synthesized. Assuming comparable product yields and loss due to characterization, approximately 0.300 - 0.350 g of BAT (**VI**) will be synthesized in the upcoming weeks.

Fig. 1 Synthesis of BAT

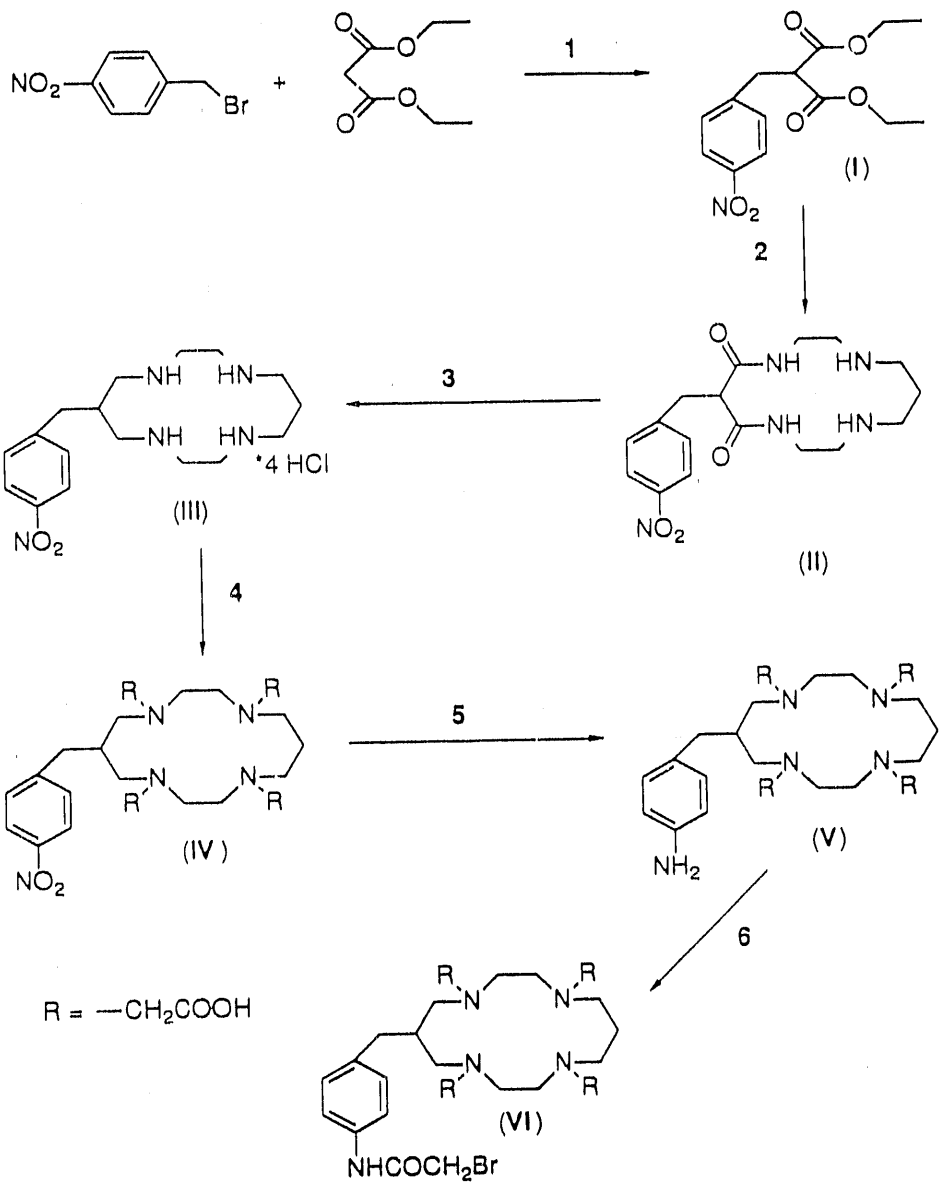

Conjugation of Lym-1-2IT-BAT and Radiolabeling with Cu-67 for Human Use

General Analytic and Laboratory Techniques

Metal free labware, buffers, and equipment were used scrupulously in the preparation and radiolabeling of antibody conjugate.

Samples examined by thin layer chromatography (TLC) were applied to a plastic-backed silica gel plate (EM Science) which is developed in 10% (w/v) ammonium acetate/methanol (1/1 v/v) solvent. In this system, unchelated metals and antibody conjugates remain at the origin while free chelates migrate to $R_f > 0.5$. The plates are imaged and quantitated with the AMBIS radioanalytic imaging system.

High-performance liquid chromatography (HPLC) of the conjugates was performed at room temperature on a 7.5 x 300 mm TSK 3000SW gel filtration column (Altex). Unlabeled immunoconjugates were eluted at 0.5 mL/min in 0.1 M sodium phosphate buffer, pH 7.0; the UV-absorbing fractions were detected at 280 nm. Cu-67 labeled immunoconjugates were eluted at 1.0 mL/min in 0.1 M sodium phosphate buffer pH 7.4, containing 0.005% NaN_3 by weight and detected by a Beckman 170 radioisotope detector.

Cellulose acetate electrophoresis (CAE) was performed with 0.05 M barbital buffer pH 8.6 for 45 minutes at 300 V.

Preparation of Lym-1-2IT-BAT

Bromoacetamidobenzyl TETA (BAT) was prepared and conjugated to Lym-1 (Damon Biotech, Needham Heights, MA) via 2-iminothiolane (2IT). Three lots (A, B, and C) of conjugate were prepared according to the methods of McCall et al.[1] The concentrations of Lym-1 (mg/mL), 2IT (mM), and BAT (mM) in the conjugation solutions were (A) 17, 1.0, and 2.0; (B) 19, 1.0, and 2.0; and (C) 11, 1.5, and 3.0. Conjugates A and B were purified and transferred to double deionized water (dd H_2O) by column centrifugation[2,3]; conjugate C was purified and transferred to dd H2O by size exclusion chromatography through a 1 x 30 cm Sephadex G-50 column. Lots A, B, and C were cobalt assayed at 1.0, 1.3, and 1.0 average available chelate sites per antibody according to the method of McCall et al. Each lot was examined by HPLC to assure that antibody conjugate aggregation was <5% in all cases. All conjugates were plunged into liquid nitrogen and stored at -70°C until immediately before use.

Mouse weight toxicity studies of each lot were conducted as follows: 20 µg of conjugate in 100 µL of 0.9 percent sterile saline was injected into each of six BALB/c mice; sterile saline alone was injected into six control mice. All mice were weighed at the time of injection and at 24, 48, 72, and 120 hours after injection. In all cases, weight gain of the conjugate-injected mice at all time points corresponded to that of the control mice.

Lym 1-2IT-BAT-Cu-67 Radiolabeling

Five lots of Cu-67 (Brookhaven and Los Alamos National Laboratories) were used to radiolabel six patient doses. Because the specific activity of the Cu-67 varied by supplier and lot, each lot was titrated against Lym-1-2IT-BAT to determine the achievable activity per unit mass of radioimmunoconjugate. A 1.5- to 2-fold excess of Cu-67 was introduced to conjugate in the complexation solution.

Radiolabeling was performed as follows: Cu-67 in 0.5 M HCl was dried on a 70 °C heat block under a gentle stream of nitrogen gas. 1.0 M ammonium citrate, pH 5.0, was added to the immunoconjugate solution such that final buffer concentration was 0.1 M; then buffered immunoconjugate was added to the dried copper. This complexation solution was allowed to incubate 30 min at room temperature. 100 mM Na_2EDTA was added to a final concentration of 10 mM. The solution was allowed to incubate an additional 10 min at room temperature. A solution of Cu-67 and *unmodified* Lym 1 was similarly challenged to determine that all nonspecifically bound copper is complexed by the EDTA.

The challenged immunoconjugate solution was purified and transferred to 0.9% sterile saline (Travenol, Deerfield, IL) by elution through an open 1 x 30 cm Sephadex G-50 column. 0.7 mL of 25% HSA (Alpha Therapeutic, Los Angeles) had previously been eluted through the column to prevent nonspecific binding of the antibody. The eluent was filtered through a Millipore 0.22 µm cartridge which had also been preconditioned with HSA. In the case of Patient 1, the challenged immunoconjugate

solution was purified and transferred to dd H_2O by column centrifugation before application to the open column. An aliquot of the radiopharmaceutical was challenged with EDTA and examined by TLC to verify the absence of nonspecifically bound copper. Protein recovery was determined using $E^{1\%}$ of 13.5 at 280 nm.[4] The preparation was diluted in sterile saline solution and stabilized with HSA such that final concentrations of Lym 1-2IT-BAT-Cu-67 and HSA were 1.0 mg/mL and 40 mg/mL, respectively; this solution was examined by HPLC, CAE, and LAL. A fixed Raji cell immunoassay according to the method of DeNardo et al.[5] was conducted to determine the immunoreactivity of the radiopharmaceutical relative to that of I-125 iodinated Lym 1.

Quality control analysis of the radioimmunoconjugate preparations is summarized in Table 1. Radioanalytic HPLC of the radiopharmaceutical showed that <10% of the Cu-67 label was complexed to aggregates. No significant amounts of radiolabeled low-molecular-weight species (e.g., EDTA-Cu-67) were detected. All radiopharmaceutical preparations displayed >90% immunoreactivity relative to I-125 iodinated Lym 1. Virtually all counts migrated as one CAE band in both cases, and all preparations were LAL negative.

Table 1. Lym-1-2IT-BAT-Cu-67 radiopharmaceutical preparations.

Patient	Conjugate lot	mCi Cu-67 per mg Lym-1-2IT-BAD	Immunoreactivity relative to Lym-1-I-125	Fraction of Cu-67 on aggregates
1	A	0.12	98%	0.01
2	B	1.0	100%	0.09
3	B	0.20	96%	0.07
4	C	1.3	>90%	0.01
5	C	0.80	92%	0.05
6	C	0.77	92%	0.05

Synthesis, characterization and properties of 1,4,8,11-Tetrakis-(2-carboxybenzyl)-1,4,8,11-tetraazacyclotetradecane-hydrochloride

1. Synthesis: This new tetra-substituted derivative of 1,4,8,11 - Tetraazacyclotetradecane (cyclam) was synthesized as shown:
Scheme 1:

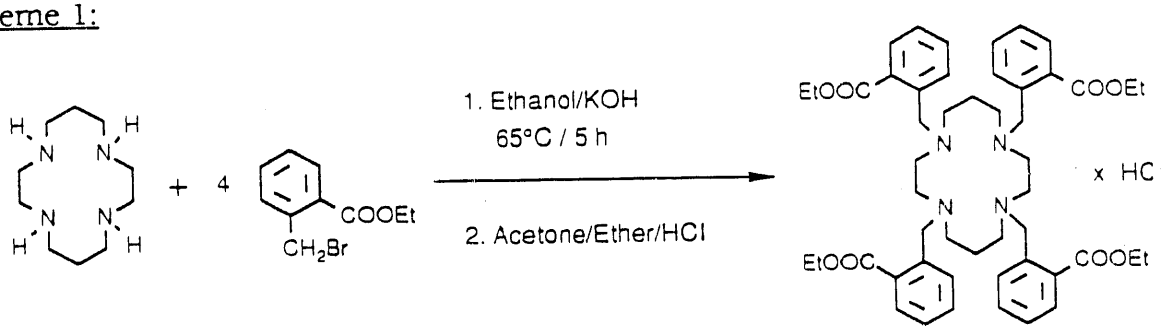

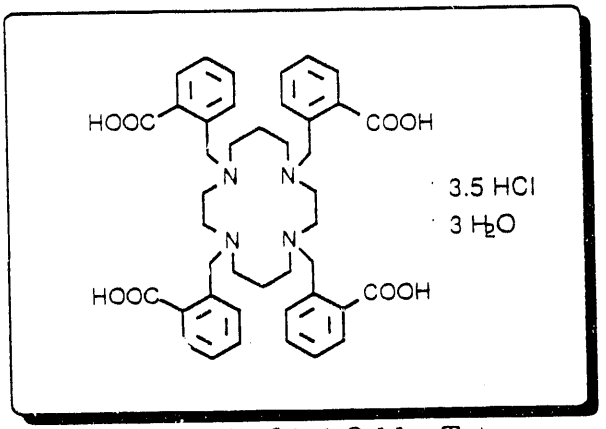

To a mixture of 1.5 g (7.5 mmol) of 1,4,8,11 - Tetraazacyclotetradecane and 2.58 g (46 mmol) solid KOH in 15 ml abs. ethanol at 65° C, 14.6 g (45 mmol) 2-Bromomethylbenzoicacid-ethylester, dissolved in 15 ml abs. ethanol, was added during 1h. The reaction mixture was stirred for another 5 h at 65° C. After cooling to 4 °C, the formed precipitate (KBr) was filtered off and the ethanol is evaporated. To the oily residue 100 ml of acetone is added. The mixture is refluxed for 15 min. and 3 ml of 36% HCl are added to form the hydrochloride. After cooling down slowly to 4 °C the precipitate is filtered off. A second portion is collected after addition of 100 ml dimethyl ether to the filtrate, saturation with HCl (g) and cooling to -30 °C. The crude intermediate was hydrolyzed in 100 ml of 18 % HCl at 110 °C for 48 h. After cooling the reaction mixture to -30 °C a colorless precipitate was formed to give 3.1 g (3.4 mmol, 45%) of product. The new macrocyclic compound was characterized by NMR, MS, IR and elemental analysis: ^{1}H NMR (D_2O/NaOD; pH* ~ 12): 1.6 - 1.8 (m, 4 H); 2.3 - 2.8 (m, 16 H); 3.7 (s, 8 H); 7.1 - 7.6 (m, 16 H). FAB-MS: m/e 738 ($M + H^+$). FT - IR: 1705 cm^{-1} (Ar-COOH). Elemental Analysis: C_{42} H_{48} N_4 $O_8 \cdot 3.5$ HCl $\cdot$ 3 H_2O, 918.54. Calculated: C: 55.20 H: 6.45 N: 6.00 CI: 13.32 O: 19.03. Found: C: 54.94 H: 6.31 N: 6.10 CI: 13.51 O: 19.16 (calculated by difference).

2. Cu(II) - complexes:
A Cu (II)-complex can easily be formed at room temperature by adding an equal amount of $CuCl_2 \cdot 2\ H_2O$ to a solution of the ligand in a methanol/water mixture (1:1) at pH~5. At lower pH (~2) the complex decomposes, which indicates that the macrocycle is in a trans- I configuration, where all sidechains point to the same side. A color change and shift to higher wavelengths above pH~8 is unusual for this type of macrocycle and can not be explained so far. It might indicate a configuration change at the nitrogen atoms. The spectroscopic data of the complex (3 mM solutions in methanol/water 1:1), at different pH values are shown in Table 1.

Table 1: Absorbance

pH	λ_{max}	$\varepsilon(\lambda_{max})$
11.7	706	245
5.0	606	133
2.3	606	decomposition

The binuclear Cu(II)-complex was crystallized an its X-ray structure solved. The macrocycle is in the trans-I configuration. Both Cu(II) cations are pentacoordinated by two nitrogen atoms of the macrocycle, two oxygen atoms of the carboxylate sidechains and a water molecule acts as a bridging ligand. The coordination geometry is in between square pyramidal and trigonal bipyramidal. The four nitrogen atoms form a perfect plane and the Cu - N and Cu - O bond lengths are in the normal range of 204.6 - 206.1 pm and 195.9 - 196.8 pm respectively. The distance of the bridging oxygen atom to Cu1 and Cu2 is 260.5 and 243.4 pm.

Large Scale Nitrobenzyl-DOTA Synthesis
The synthesis of nitrobenzyl-DOTA, a ten step synthesis, was done in our lab according to the published procedure (Min Moi et al., J. Am. Chem. Soc. 110 [1988] 6266).The starting material, either (L)- or (D)-Phenylalanine gives nitrobenzyl-(S)- or (R)-DOTA. However, some yields are very relatively low, and a HPLC purification was necessary for the last four steps. The preparations done previously gave final yields of 0.9-1.0%, resulting in about 1.5 g of nitrobenzyl-DOTA. This synthesis report describes the first large scale synthesis of nitrobenzyl-DOTA. In addition, the yields of most of the steps were improved.
The synthesis of the first five precursors of nitrobenzyl-DOTA was done essentially as described. Changes were made in the work-up of the reaction mixtures and the final purifications. The reduction of p-Nitrophenylalanylglycylglycylglycine (5) to 11-p-nitrobenzyl-3,6,9,12-tetraazadodecanol (6) was done on a 250 ml 1 M Borane-THF scale, which allows the reduction of about 7.2 g of (6). However, the improved synthesis of steps 1-5 gave 133.7 g of (6). This would have required about 17 reductions (approximately eight weeks) compared to the usual five. A reduction apparatus therefore had to be designed to do reductions on larger scale. The apparatus was carefully tested, especially the influence of a possible higher hydrogen pressure was investigated. A magnetic stirrer with a speed control system was used to guarantee effective stirring of the mixture. Reductions using up to 1600 ml 1 M Borane-THF can and have been done safely. The work-up of the reduction product was also remarkably improved; purification via a silica gel column chromatography is no longer necessary. Compound (6) can be obtained in high quality and almost quantitative yield.

It was not possible to increase the yields of the tosylation drastically, although numerous reaction conditions were investigated. A HPLC purification of the crude product (7) cannot be avoided due to the high number of byproducts. Most of the yellow material could be removed by open silica gel chromatography which made it possible to use a less sensitive filter in the UV detector of the HPLC (generally absorbance is detected at 254 nm; for this purification a 340 nm filter could be used) and to inject larger amounts to cut the number of injections dramatically. However, the total run time is still 162 hours (245 injections· 130 l HPLC solvents; 185 mg product per injection).
For the purification of (9), HPLC is no longer necessary since (9) can be recrystallized in good quality on this scale. This also eliminates an expensive HPLC procedure. The yields of the detosylation and the final alkylation have also been improved, but HPLC purification is still recommended. Both HPLC purifications can be done using aqueous conditions and the amount of HPLC methanol or acetonitrile necessary for the gradients is relatively small.

Description of the synthesis

Yields are not given when the material of two or more preparations was pooled for final purification. For total yields of each step see Table II.

1. (S)-p-Nitrophenylalanine: (S)-Phenylalanine (80 g, 0.48 mol) was dissolved in 215 ml concentrated sulfuric acid over the course of 5 h at 0 °C. 27 ml Nitric acid were added slowly over the course of 2 hours at 4-8 C. On neutralization, (S)-p-nitrophenylalanine, (1), precipitated. The precipitate was collected, and recrystallized from water. Yield: 61.63 g (61%). ^{1}H NMR (300 MHz), D_2O, pH 6) 3.18 (q, 1H), 3.23 (q, 1H), 3.90 (t, 1H), 7.40 (d, 2H), 8.10 (d, 2H).

2. N-(tert-Butoxycarbonyl)-(R)-p-nitrophenylalanine: Compound (1) above (61.63 g, 293.2 mmol in 176 ml H2O) was reacted with BOC-ON (79.5 g, 105 mmol) in 171 ml dioxane and 62 ml triethylamine (4 hr, room temperature, nitrogen atmosphere). The reaction mixture was poured into 500 ml water and 400 ml ether and the pH adjusted to 1 with 6 M HCl. The solution was extracted with ethyl acetate, and the extracts taken to dryness. The yellow material was dissolved in 300 ml ether, the solvent removed under reduced pressure and the residue was lyophilized to give the product, N-(tert-butoxycarbonyl)-(R)-p-nitrophenylalanine (2) as a white powder. Yield: 18.9 g (64%).
^{1}H NMR (300 MHz, $CDCl_3$) 1.30 (d, 9H), 3.10 (m, 2H), 4.50 (q, 1H), 7.40 (d, 2H), 9.80 (s, 1H).

3. N-(tert-Butoxycarbonyl)-(S)-p-nitrophenylalanine-N-hydroxysuccinimide ester: N-Hydroxysuccinimide (29 g, 252 mmol) was added to a solution of compound (2) (77.97 g, 252 mmol) and DCC (57 g, 275 mmol) in 1250 ml dioxane (room temperature, 17 hr, under nitrogen). The resulting precipitate was filtered off and the filtrate taken to dryness. The residue was dissolved in 1000 ml 2-propanol and the undissolved material was filtered off. The filtrate was taken to dryness, giving N-tert-butoxycarbonyl)-(S)-p-nitrophenylalanine-N-hydroxysuccinimide ester (3). Yield 87.03 g (81.5%).
^{1}H NMR (300 MHz, $CDCl_3$) 1.40 (s, 9H), 2.90 (s, 4H), 3.40 (m, 2H), 5.00 (s, 1H), 7.50 (d, 2H), 8.20 (d, 2H).

4. N-(tert-Butoxycarbonyl)-(R)-p-nitrophenylalanylglycylglycylglycine: Compound (3) (93.00 g, 219 mmol) in 415 ml DMF was added to a solution of 58.25 g triglycine and 34.42 g sodium bicarbonate in 820 ml and the solution stirred for 5 h at room temperature (nitrogen atmosphere). The reaction mixture was filtered and

1770 ml water was added. The product, N-(tert-butoxycarbonyl)-(S)-nitrophenylglycylglycylglycine, (4), was precipitated from solution by the addition of concentrated HCl (final pH 1). The precipitate was aged at 4 °C for 12 h, filtered off, washed with ether and dried in a desiccator under reduced pressure. Yield 104.09 g (99%).

^{1}H NMR (300 MHz, D_2O, pH 11) 1.10 (s, 3H), 1.25 (s, 6H), 3.15 (m, 2H0, 3.65 (s, 3H), 3.85 (s, 3H), 4.40 (m, 1H) 7.25 (d, 2H), 8.05 (d, 2H); FABMS m/e=504 ($m=Na^+$)

5. (S)-p-Nitrophenylalanylglycylglycylglycine: Compound (4) was dissolved in trifluoroacetic acid at 0 °C and stirred for one hour. The solvent was removed under reduced pressure to give (S)-p-nitrophenylalanylglycylglycylglycine (5) as the TFA salt in quantitative yield. The TFA-salt (5) is very hygroscopic. The preparation of (5) was always done immediately before the reduction or the sample was stored under high vacuum.

FAB-MS m/e=382 ($m=H^+$).

6. & 7. (S)-11-p-Nitrobenzyl-3,6,9,12-tetraazadodecanol hydrochloride (6) and free base (7): Compound (5) (44.52 g), was dissolved in 420 ml freshly distilled THF and after cooling to 0 °C, 1600 ml 1 M Borane-THF complex (1600 mmol) was slowly added. The mixture was refluxed for 17 h, cooled to 0 °C, quenched with 200 ml methanol, saturated with HCl and refluxed again for 17 h. The solvent was removed by evaporation under reduced pressure. The remaining viscous colorless solution was decanted and the white gummy precipitate was washed with chloroform, dissolved in 1000 ml water and washed again with 3x200 ml chloroform. The solvent was evaporated under reduced pressure and lyophilized to give (6) as a white powder. The resulting hydrochloride salt (6) was taken up in NaOH solution (to pH 10). This basic solution was continuously extracted with chloroform for 8 h. The organic layer was taken to dryness under reduced pressure to give (S)-11-p-nitrobenzyl-3,6,9,12-tetraazadodecanol (7). (7) ^{1}H NMR (300 MHz, D_2O, pH 11): 2.25 (br.s, 6H), 2.50-3.00 (m, 14H), 3.10 (m, 1H), 3.60 (t, 2H), 7.35 (d, 2H), 8.15 (d, 2H); FTIR no carbonyl absorption from 1610-1700; FABMS m/e ($M=H^+$) 326

8. (S)-11-p-Nitrobenzyl-N,N',N'',N''', O-(pentatoluenesulfonyl)-3,6,9,12-tetraazadodecanol: Compound (7) (30.9 g, 94 mmol) was dissolved in 470 ml acetonitrile, 240 ml triethylamine and 240 ml methylene chloride. 90.0 g (471 mmol) p-toluenesulfonyl-chloride was added and the mixture was stirred for 5 h under a nitrogen atmosphere. The solvent was removed under reduced pressure and the residue taken up in chloroform, washed with HCl and purified by normal phase HPLC to give the product (S)-11-p-Nitrobenzyl-N,N',N'',N''', O-(pentatoluenesulfonyl)-3,6,9,12-tetraazadodecanol (8).

^{1}H NMR (300 MHz, $CDCl_3$): 2.30 (S, 3H), 2.50 (M,12H), 2.60-3.50 (M, 14H), 3.75 (M, 1H), 4.20 (t, 2H), 5.30 (d, 1H), 7.00-7.90 (m, 24H); High resolution FABMS m/e=1096.263 $(M+H)^+$ calcd; found=1096.265.

9. (S)-2-p-Nitrobenzyl-N,N',N'',N'''-(tetratoluenesulfonyl)-1,4,7,10-tetraazacylododecane: Compound (8) (45.43 g, 41.5 mmol) was dissolved in 4200 ml DMF, Cesium carbonate (13.4 g, 42 mmol) added and the mixture stirred at 60 °C for 5 h under nitrogen atmosphere. The solvent was removed by evaporation under reduced pressure, the residue taken up into chloroform and washed with 0.1 N HCl (3x250 ml). The solvent was again removed under reduced pressure to give the crude compound (9). The residue was purified by open silica gel chromatography (4x8 cm, eluent chloroform), the volume reduced and methanol and ethyl acetate was

added to precipitate the (S)-2-p-Nitrobenzyl-N,N',N",N"'-(tetratoluenesulfonyl)-1,4,7,10-tetraazacylododecane (9) after cooling to 4 °C. Yield: 22.05 g (58%). ^{1}H NMR (300 MHz, $CDCl_3$): 2.40-2.60 (m, 12H0, 3.00-4.20 (m, 16H), 4.50 (m, 1H), 7.00-7.50 (m, 12H), 7.60-7.90 (m, 6H, 8.15 (d, 2H); FABMS m/e calcd ($M+H^+$) 924.24; found 924.25.

10. (S)-2-p-Nitrobenzyl-1,4,7,10-tetraazacyclododecane: Compound (9) (13.03 g, 14.1 mmol) was dissolved in 600 ml concentrated sulfuric acid and 22.5 g phenol was added. The mixture was heated to 100 °C and stirred for 56 h under nitrogen atmosphere. The mixture was poured into 2000 ml ice and neutralized with about 3.3 kg barium hydroxide. The barium hydroxide precipitate was aged at 4 °C for 12 h and filtered off. The remaining solution (9.5 l) was evaporated to a small volume (about 300 ml) under reduced pressure and purified by reversed phase HPLC to give the product (S)-2-p-Nitrobenzyl-1,4,7,10-tetraazacyclododecane (10). ^{1}H NMR (300 MHz, D_2O, pH 2): 2.80-3.50 (m,17H), 7.50 (d, 2H), 8.20 (d, 2H); FAB-MS m/e calcd ($M+H^+$) 308.210; found 308.209.

11. (S)-2-p-Nitrobenzyl-1,4,7,10-tetraazacyclododecane-N,N'.N",N"'-tetraacetic acid: Bromoacetic acid (10.14 g, 73.0 mmol) was added to a solution of compound (10) (4.48 g, 14.6 mmol) in 45 ml water at pH 11. The mixture was stirred at 70 °C, while the pH was maintained at 10 with 3 N NaOH using a pH-stat.. After 5 h the solution was neutralized with 6 N HCl and purified by reversed phase HPLC to give the product (S)-2-p-Nitrobenzyl-1,4,7,10-tetraazacyclododecane-N,N'.N",N"'-tetraacetic acid (11).

^{1}H NMR (300 MHz, D_2O, pH 10) 2.75-4.00 (complex multiplet, 25H), 7.50 (t, 2H); 8.20 (d, 2H); High resolution FAB-MS m/e=540.229 ($M+H^+$), found 540.

Table I: Synthesis of Nitrobenzyl-(S)-DOTA

1. Nitration of (S)-Phenylalanine			
Starting material:	80.00 g	(484.3 mmol)	
Yield:	61.63 g	(293.2 mmol)	60.5%
2. BOC Protection of (S)-p-Nitrophenylalanine			
Starting material:	61.63 g	(293.2 mmol)	
Yield:	77.97 g	(251.8 mmol)	85.9%
3. NHS Activation of the protected amino acid			
Starting material:	77.97 g	(251.8 mmol)	
Yield:	87.03 g	(205.3 mmol)	81.5%
4. Synthesis of the tetrapeptide			
Starting material:	93.00 g	(219.3 mmol)	
Yield:	104.09 g	(216.0 mmol)	98.6%
5. Deprotection of the tetrapeptide			
Starting Material:	103.72 g	(215.3 mmol)	
Yield:	133.66 g	(213.5 mmol)	99.0%
6. Reduction of the tetrapeptide			
Starting material:	133.66 g	(213.5 mmol)	
Yield:	100.19 g	(197.3 mmol)	92.4%
7. Synthesis of the free amine of the reduced peptide			
Starting Material:	91.93 g	(181.1 mmol)	
Yield:	55.93	(171.9 mmol)	94.9%

8. Tosylation			
Starting material:	52.36 g	(160.8 mmol)	
Yield:	45.43 g	(41.5 mmol)	25.8%
9. Cyclization			
Starting material:	45.43 g	(41.5 mmol)	
Yield:	22.05 g	(23.9 mmol)	57.6%
10. Detosylation			
Starting material:	22.03 g	(23.8 mmol)	
Yield:	8.83 g	(16.6 mmol)	69.7%
11. Alkylation			
Starting material:	8.83 g	(16.6 mmol)	
Yield:	6.50 g	(12.05 mmol)	72.5%
Total yield:	**484.3 mmol =>**	**12.05 mmol =>>**	**2.50%**
Yield calculated for the single steps 1.-11.			**2.72%**

Quality control
The purity of the synthesized nitrobenzyl-(S)-DOTA was carefully checked by FAB-MS, ^{1}H-NMR and by analytical HPLC. Analytical HPLC revealed single peaks with no impurities detectable. Metal Binding Assays were performed with Co-57 (Table II).

Table II: Characterization of Nitrobenzyl-(S)-DOTA Preparations:

	nbz-(S)-DOTA according to mass	nbz-(S)-DOTA according to metal binding assay
OR 93	2.32 g	2.32 g
OR 94	3.71 g	3.32 g
OR 93/4	0.37 g	0.28 g
OR 94X	0.13 g	no assay
Total	6.53 g	5.93 g

For a 10 mg/ml sample of nitrobenzyl-DOTA one would expect to obtain a 18.5 mM solution (based on weight).

>> Concentrations by UV analysis (NO_2-C_6H_4-, ε = 9050 $M^{-1}cm^{-1}$ at 280 nm)

OR 93	17.05 mM	92%
OR 94	14.27 mM	77%
OR 93/4	13.34 mM	72%

>> Concentrations by Co-57 metal binding analysis
(0.1 M NH_4OAc, pH=9, 30 min, RT)

OR 93	18.56 mM±1.57	100%
OR 94	16.60 mM±0.03	90%
OR 93/4	13.94 mM±0.40	75%

>>MS
FAB-MS m/e: 540 (M+H+), 562 (M+Na+)
CF-FABMS m/e: 540 (M+H+), 562 (M+Na+), CF FABMS shows less M+Na+

Results of Labeling DOTA with Yttrium-88

1. General description

The results of labeling DOTA with Y-88 were analyzed by the TLC assay. Y-88 was purchased from Los Alamos National Laboratory. The solution of Y-88 was dried under IR lamp in the air and then dissolved in the buffer to give a 2 μM Y-88 solution. DOTA (ammonium salt) was purchased from Parish Chemical Co. The purity was 88.9% ± 1.7%, determined by Co-57 binding assay. A series of DOTA solutions of varying concentration was prepared. The same volume of Y-88 solution and DOTA solution was mixed and the mixture was incubated under specified conditions. The final concentration of Y-88 was 1 μM and the molar ratio of DOTA to Y-88 was 1, 5, 10, 30, 70, 100, 300, 700, 1000, and 10000. Ammonium acetate was used as the buffer in all the experiments.

2. Experiments and Results

(1) Buffer Concentration Dependence Studies

The binding assays of Y-DOTA were studied at different concentrations of ammonium acetate: 0.1 M, 1 M, 2 M, 3 M, 5 M, 7 M, and 10 M at RT. The pH of all the solutions was approximately 7. The best results were:

a. Y-88 received on 7/10/91: 92% of Y was complexed by DOTA at a ratio [DOTA]/[Y-88] = 100 in 3 h, and 86% at [DOTA]/[Y-88] = 70 in 24 h in 2 M ammonium acetate, pH = 7.16.

b. Y-88 received on 9/20/91: 84% of Y was taken by DOTA at [DOTA]/[Y-88] = 70 in 1 h, 99% at [DOTA]/[Y-88] = 70 in 3.5 hrs, and 58% at [DOTA]/[Y-88] = 30 in 125 hrs in 2 M ammonium acetate, pH = 7.16.

(2) pH Dependence Studies

The binding assays of Y-DOTA were performed in 2 M ammonium acetate at three pH's: 7.16, 8.02, and 9.02 respectively. The best result was found at pH 7.16.

(3) Temperature Dependence Studies

The binding of yttrium to DOTA was studied at room temperature and 80 °C in 2 M ammonium acetate, pH=7.16. The results were improved at high temperature: 53% of Y was taken by DOTA at [DOTA]/[Y-88] = 30 in 3 hrs, 87% at [DOTA]/[Y-88] = 30 in 20 hrs (y-88 received on 9/20/91).

(4) Y-88 Purification

Y-88 purification was attempted by several different methods which included: 1) liquid-liquid TOPO extraction; 2) TOPO extraction column; and 3) cation-exchange column. Unfortunately, all the attempts failed to improve on the purity of Y-88 as received.

3. Summary

The best conditions for preparing Y-DOTA are listed below:

Buffer	pH	Temp.	[DOTA]/[Y]	time, h	% Y chelated*
2 M ammonium acetate	7.16	room T	70	3.5	99
			30	125	58
		80 °C	30	3	53
			30	20	87

* Results based on Y-88 received on 9/20/91, without further purification.

Literature Cited

[NOTE: some references appear more than once. Our word processor requires a new number for each citation.]

1 M. J. McCall, H. Diril, and C. F. Meares, Simplified Method for Conjugating Macrocyclic Chelating Agents to Antibodies via 2-Iminothiolane, *Bioconjugate Chem.* **1:** 222-226 (1990).

2 C. F. Meares, M. J. McCall, D. T. Reardan, D. A. Goodwin, C. I. Diamanti, and M. McTigue, Conjugation of Antibodies with Bifunctional Chelating Agents: Isothiocyanate and Bromoacetamide Reagents, Methods of Analysis and Subsequent Addition of Metal Ions, *Anal. Biochem.* **142:** 68-78 (1984).

3 H. S. Penefsky, A Centrifuged-Column Procedure for the Measurement of Ligand Binding by Beef Heart F1, *Methods Enzymol.* **56:** 527-530 (1979).

4 E. Harlow and D. Lane, Antibodies: A Laboratory Manual p 673, Cold Spring Harbor Laboratory, Cold Spring Harbor, NY (1988).

5 S. J. DeNardo, J.-S. Peng, G. L. DeNardo, S. L. Mills, and A. L. Epstein, Immunochemical Aspects of Monoclonal Antibodies Important for Radiopharmaceutical Development, *Nucl. Med. Biol.* **13:** 303-310 (1986).

LITERATURE CITED

1. G.L. DeNardo, A. Raventos, H.Hines, P.O. Schelbe, D.J. Macey, M.T. Hayes and S.J. DeNardo. Requirements for a treatment planning system for radioimmunotherapy. Internatl. J. Rad. Onc. Biol. Phys. 11:335-345, 1985.
2. J.A. Carrasquillo, H.A. Krohn, P. Beaumier, R.W. McGuffin, J.Brown, K.E. Hellstrom, I. Hellstrom, S.M.Larson. Diagnosis of and therapy for solid tumors with radiolabeled antibodies and immune fragments. Cancer Treat. Repts. 68:317-318, 1984.
3. J.F. Chatal, J.C. Saccavini, P. Fumoleau, J. Y. Douillard, C. Curtet, M. Kremer, B. LeMevel, H. Koprowski. Immunoscintigraphy of colon carcinoma. J. Nuc. Med. 25:307-314, 1984.
4. F.H. DeLand, D.M. Goldenberg. In vivo cancer diagnosis by radioimmunodetection. In: Radioimmunoimaging and Radioimmunotherapy. S.W. Burchiel and B.A. Rhodes, eds., Elsevier Science Publishing Co. 1983.
5. G.L. DeNardo, S.J. DeNardo, D.J. Macey. Cancer treatment with radioactive labeled antibodies. In: Nuclear Medicine in Clinical Oncology, C. Winkler, ed., Springer-Verlag, Berlin, Heidelberg, 1986.
6. A.A. Epenetos. Clinical results with regional antibody-guided irradiation. Cancer Drug Delivery 2:233, 1985.
7. A.A. Epentos, S. Mather, M.Granowska, C.C. Nimmon, L.R. Hawkins, K.E. Britton, J.Shepherd, J. Taylor-Papadiminitriou, H. Durbin, J.S. Malpas, W.F. Bodmer. Targeting of Iodine-123 labeled tumor associated monoclonal antibodies to ovarian, breast and gastrointestinal tumors. Lancer 2:999-1004, 1982.
8. A.L. Epstein, A.M. Zimmer, S.M. Spies, S. Mills, G. DeNardo, S. DeNardo. Radioimmunodetection of human B cell lymphomas with a radiolabeled tumor-specific monoclonal antibody (Lym-1). In: Malignant Lymphomas and Hodgkins disease: Experimental and Therapeutic Advances, F. Cavalli, G. Bonaddona, M. Rozeneweig, eds., Martinus Nijhoff Publishing, Boston, 1985.
9. D.M. Goldenberg, F. DeLand, E. Kim, S. Bennett, F.J. Primus, J.R. vanNagell, N. Estes, P. DeSimnoe, P. Rayburn. Use of radiolabeled antibodies to carcinoembryonic antigen for the detection and localization of diverse cancers by external photoscanning. New Eng. J. Med. 298:1384-1388, 1978.
10. S.E. Halpern, R.O. Dillman, K.F. Witztum, J.F. Shega, P.L. Hagan, W.M.Burrows, J.B. Dillman, J.L. Clutter, R.E. Sobol, J.M. Frincke, R.M. Bartholomew, G.S. David, D.J. Carlo. Radioimmunodetection of melanoma utilizing In-111. 96.5 monoclonal antibody: A preliminary report. Radiology 155:493-499, 1985.
11. J-P. Mach, J-F Chatal, J-D Lumbroso, F. Buchegger, M. Forni, J. Ritschard, C. Berche, J-Y Douillard, S. Carrel: Tumor localization in patients by radiolabeled antibodies against colon carcinoma. Cancer Res. 43:5593-5600, 1983.
12. J.L. Murray, M.G. Rosenblum, R.E. Sobol, R.M. Bartholomew, C.E. Plager, T.P. Haynie, M.F. Jahns, J.H. Glenn, L. Lamki, R.S. Benjamin, N. Papadoupoulos, A.W. Boddie, J.M. Frincke, G.S. David, D.J. Carlo, E.M. Hersh. Radioimmunoimaging in malignant melanoma with In-labeled monoclonal antibody 96.5. Cancer Res. 45:2382-2386, 1985.
13. L.F. O'Grady, G.L. DeNardo, S.J. DeNardo. Radiolabeled monoclonal antibodies for the detection of cancer. Am. J. Physiologic Imaging I:44-53, 1986.
14. S.E. Order. Monoclonal antibodies: Potential role in radiation therapy and oncology. Internatl. J. Rad. Onc. Biol. Phys. 8:1193-1201, 1982.
15. M.G. Rosenblum, J.L. Murray, T.P. Haynie, H.J. Glenn, M.F. Jahns, R.S. Benjamin, J.M. Frincke, D.J. Carlo, E.M. Hersh. Pharmacokinetics of 111-In labeled anti-P97 monoclonal antibody in patients with metastatic malignant melanoma. Cancer Res. 45:2382-2386, 1985.
16. G.L. DeNardo, S.J. DeNardo, J-S Peng, L.F. O'Grady, S.L. Mills, A.L. Epstein, R.D. Cardiff. Evidence of a saturable hepatic receptor for mouse monoclonal antibodies. J Nuc. Med. 26:67, 1985.
17. S.J. DeNardo, G.L. DeNardo, L.F. O'Grady, J-S Peng, D.J. Macey, S.L. Mills, R.D. Cardiff, A.L. Epstein. Human Kinetic distribution of I-123 intact antibody. J. Nuc. Med. 26:112, 1985.
18. K. Koizumi, G.L. DeNardo, S.J. DeNardo, J-S Peng, D.J. Macey, K.Hisada, N. Tonami. Multicompartmental analysis of the kinetics of monoclonal antibody in cancer patients. J. Nuc. Med. 27:1243-1254, 1986.
19. S.J. DeNardo, G.L. DeNardo, J-S Peng, D. Colcher. Monoclonal antibody radiopharmaceuticals for cancer radioimmunotherapy. In: Radioimmunoimaging and Radioimmunotherapy, S. Burchiel, B. Rhodes, eds., Elsevier Publishing, New

20. D.J. Macey, R. Marshall. The lungs, In: Computed Emission Tomography, P.J. Ell and B.L. Holman, eds., Oxford University Press, New York, Toronto, 495-520, 1982.
21. A.L. Epstein, R.J. Marder, J.N. Winter, E. Stathopoulos, F-M Chen, J.W. Parker, C.R. Taylor. Two new monoclonal antibodies, Lym-1 and Lym-2, reactive with human B lymphocytes and derived tumors with immunodiagnostic and immunotherapeutic potential. Cancer Res., In press.
22. D.J. Macey, R. Marshall. Absolute quantitation of radiotracer uptake in the lungs using a gamma camera. J. Nuc. Med. 23:731-734, 1982.
23. D.J. Macey, G.L. DeNardo, S.J. DeNardo, H.H. Hines. Comparison of low and medium-energy collimators for SPECT imaging with Iodine-123 labeled antibodies. J. Nuc. Med. 27:1467-1474, 1986.
24. F.B. Atkins, R.N. Beck, P.B. Hoffer, D. Palmer. Dependence of optimum baseline setting on scatter fraction and detector response function in medical radionuclide imaging, IAEA, Vienna, 1977.
25. J.W. Beck, R.J. Jaszczak, R.E. Coleman, C.F. Starmer, L.W. Nolte. Analysis of SPECT including scatter and attenuation using sophisticated Monte Carlo modeling methods. IEEE Trans. Nuc. Sci. 506-511, 1982.
26. T.F. Budinger, S.E. Derenzo, W.L. Greenberg, G.T. Gullberg, R.H. Huesman. Quantitative potentials of dynamic emission computed tomography. J. Nuc. Med. 19:309-315, 1978.
27. T.F. Budinger, G.T. Gullberg. Transverse section reconstruction of gamma-ray emitting radionuclides in patients. In: Reconstruction Tomography in Diagnostic Radiology and Nuclear Medicine, M.M. Ter-Pogossian, M.E. Phelps, G.L. Brownell, et. al, eds., University Park Press, Baltimore, 1977.
28. R.J. Jaszczak, L.T. Chang, N.A. Stein, F.E. Moore. Whole body single-photon emission computed tomography using dual, large-field-of view scintillation cameras. Phys. Med. Biol. 24:1123-1143, 1979.
29. R.J. Jaszczak, R.E. Coleman, F.R. Whitehead. Physical factors affecting quantitative measurements using camera based SPECT, IEEE Trans. Nuc. Sci. 28:69-80, 1981.
30. J.W. Keyes. Perspectives on tomography. J. Nuc. Med. 23:633-640, 1982.
31. G. Muehllehner, J.G. Colsher, E.W. Stoub. Correction for field nonuniformity in scintillation camera through removal of spatial distortion. J. Nuc. Med. 21:771-776, 1980.
32. M.E. Phelps. Emission computed tomography. Seminars in Nuc. Med. 7:337-365, 1977.
33. R.J. Jaszczak, K.L. Greer, C.E. Floyd, C.C. Harris, R.E. Coleman. Improved SPECT quantification using compensation for scattered photons. J. Nuc. Med. 25:893-900, 1984.
34. B. Axelson, P. Maaki, A. Israelson. Subtraction of compton-scattered photons in single photon emission computerized tomography. J. Nuc. Med. 25:105, 1984.
35. D.J. Macey, G.L. DeNardo, S.J. DeNardo. A calibration phantom for absolute quantitation of radionuclide uptake by SPECT. J. Nuc. Med. 25:105, 1984.
36. L.T. Chang. A method for attenuation correction in radionuclide computed tomography system. IEEE Trans. Nuc. Sci. NS-25(2):638-643, 1978.
37. D.J. Macey, G.L. DeNardo, S.J. DeNardo, A.J. Seibert. A modified post processing correction matrix for SPECT. SPIE 671:189-192, 1986. Physics and engineering of computerized multidimensional imaging and processing.
38. D.J. Macey, G.L. DeNardo, S.J. DeNardo. Comparison of three boundary detection methods for SPECT using compton scattered photons. J. Nucl.Med. 29:203-207, 1988.
39. Pochin, EE, Cunningham RM, Hilton, G: Quantitative measurements of radioiodine retention in thyroid carcinoma. Journal of Clinical Endocrinology & Metabolism 14:1300, 1954.
40. Seidlin, SM, Yalow, AA, Siegel, E: Blood radioiodine concentration and blood radiation dosage during I-131 therapy for metastatic thyroid carcinoma. Journal of Clinical Endocrinology & Metabolism 12:1197, 1952.
41. Hays, MT: Kinetics of the human thyroid trap-experience in normal subjects and in thyroid disease. Journal of Nuclear Medicine 20(3):219-223, 1979.
42. Hays, MT: J.Nucl. Med 23:176-179, 1982.
43. Berger, MJ: Distribution of absorbed dose around point sources of electron and beta particles in water and other media. MIRD Pamphlet #7.
44. Spencer, LV: Energy dissipation of fast electrons. NBS Monograph 1, 1959.
45. MIRD Journal of Nuclear Medicine Supplement #1, 9-14, February 1968.
46. Lovinger, R; Berman M: A formulism for calculation of absorbed does from radionuclides. Physics in Medicine and Biology 13(2):1968.

47. Welch, Patchen, Welch: Fundamentals of the Tracer Method. W.B. Saunders Co., 178-183, 1972.
48. Berman, Kinetic Models, MIRD #12.
49. Loevinger, R, Berman, M: A revised schema for calculating the absorbed dose from biologically distributed radionuclides, NM/MIRD Pamphlet No.1, Society of Nuclear Medicine, March 1976.
50. Scheibe, P, Yoshikawa, B: Inputs for dose calculations from compartmental modes. Journal of Nuclear Medicine 15(11):1025.
51. Scheibe, PO, Thomas, AJ: Separating changes in flow from changes in receptor binding by pharmacokinetic modeling, In Receptor Binding Radiotracers, Volume X in the Uniscience Series: Radiotracers in Biology and Medicine, CRC Press, 1980.
52. Vera, DR: Design and Development of a receptor-based hepatic radio-pharmacokinetic system. University of California Doctoral Thesis, June 1982.
53. Breiman, RS, Beck, JW, Korobkin, M., et al: Volume determinations using computed tomography. AJR 138:329-333, February 1982.
54. Henderson, JM, Heymsfield, SB, Horowitz, J, Kutner, MH: Measurement of liver and spleen volume by computed tomography. Radiology 141:525-527, November 1981.
55. Moss, AA, Friedman, MA, Brito, AC: Determination of liver, kidney and spleen volumes by computed tomography: an experimental study in dogs. Journal of Computer Assisted Tomography 5(1):12-14, February 1981.
56. Reid, MH: CT of organ and lesion size: Measurement for diagnosis and therapy evaluation. In: MH Reid (ed.) Advances in Medical Imaging, 1982, pgs. 63-72.
57. Rollo, FD, DeLand, FH: The determination of live mass from radionuclide images. Radiology 91(6):1191-1194, December 1968.
58. Eikman, EA, Mack, GA, Jain, VK, Madden, JA: Computer-assisted livermass estimation from gamma-camera images. Journal of Nuclear Medicine 20: 144-148, 1979.
59. Larson, SM, Tuel, SH, Moores, KD, Nelp, WB: Dimensions of the normal adult spleen scan and prediction of spleen weight. Journal of Nuclear Medicine 12(3): 123-126, March 1971.
60. Kan, MK and GB Hopkins: Measurement of liver volume by emission computed tomography. Journal of Nuclear Medicine 20: 514-520, 1979.
61. Yamamoto, K, Mukai, T, Kinoshita, R, Minato, K, Tamaki, N, Ishii, Y and K Torizuka. In vivo measurement of effective liver volume by emission computed tomography. Journal of Nuclear Medicine 20: 514-520, 1979.
62. Rockoff, SD, Goodenough, DJ and KR McIntire: Theoretical limitations in the immunodiagnostic imaging of cancer with computed tomography anc nuclear scanning. Cancer Research 40: 3054-3058, 1980.
63. Budinger, TF: Physical attributes of single-photon tomography. Journal of Nuclear Medicine 21:579-592, 1980.
64. Kuhl, De, Edwards, RQ, Ricci, AR, et al: Quantitative section scanning using orthogonal tangent correction. Journal of Nuclear Medicine 14: 196-200, 1973.
65. Hoffman, EJ, Huang, SC, Phelps, ME: Quantitation in positron emission computed tomography: 1. Effect of object size. Journal of Computer Assisted Tomography 3: 299-308, 1979.
66. Holman, BL: Quantitative single-photon ECT: A revolution for the 80s? Applied Radiology/NM, March/April 1982.
67. Kuhl, DE, Barrio, JR, Huang, S-C, Selin, C, Ackermann, RF, Lear, JL, Wu, JL, Lin, TH, ME Phelps: Quantifying local cerebral blood flow by N-isopropyl-p-{^{123}I}Iodoamphetamine (IMP) tomography. Journal of Nuclear Medicine 23: 196-203, 1982.
68. Ahluwalia, BD: Tomographic methods in Nuclear Medicine, ed., Pub: CRC Press, 1989.
69. Howell, RW, et al. Medical Physics 16(1): 66-74, 1989
70. Kowk, CS, et al. Medical Physics 12(4): 405-412, 1985.
71. Kircos, LT, et al. Journal of Nuclear Medicine 28: 334-341, 1987.
72. Loevinger, R, et al. MIRD Pamphlet No.1, N.Y., 1976.
73. Ott, B, et al. The Physics of Medical Imaging, ed: S. Webb, Pub: Adam Hilger, Bristol, pp142-309, 1988.
74. Phelps, ME. Positron emmission tomography, ed., NY, Raven, 1986.
75. Sorenson, JA, et al. Physics in Nuclear Medicine, 2nd ed., Grune & Stratton, p.234-236 and 280-283, 1987.
76. Tsui, BMW. Computer & Instrumentation Council News Letter, SNM, Vol.1, No.5, 1990.

77. Webb, S. The Physics of Med. Imaging, ed., Pub: Adam Hilger, Bristol, 1988.
78. Webb, S, et al. Recent Development in Med. & Biomed. Imaging, ed: RP Clark, Pub:Tyler & Francis, 1986.
79. Yanch, J, et al. Proce. 10th Informal Processing in Med. Imaging Conference. Utrecht, ed: ^A Viergever, 1987.
80. Yanch, J, et al. IEEE Trans. Nuclear Science, 7: 13-20, 1988.
81. Zanzonico, PB, et al. Seminar in Nuclear Medicine., vol. XIX, No.1: 42-61, 1989.
82. Siegel, JA, Wessels, BW, Watson, EE, et al. Bone marrow dosimetry and toxicity for radioimmunotherapy. Antibody Immunoconjugates, and Radiopharmaceuticals 3(4): 213-234, 1990.
83. Stabin, MG. Marrow dose calculation: Development and practice. Antibody Immunoconjugates, and Radiopharmaceuticals 3(4): 239-246, 1990.
84. Eckerman, KF. Dosimetry of skeletal tissues: Report on ORNL efforts. Antibody Immunoconjugates, and Radiopharmaceuticals 3(4): 247-250, 1990.
85. Kwok, CS. Backscattering of low energy electrons at bone/bone marrow interfaces. Antibody Immunoconjugates, and Radiopharmaceuticals 3(4): 251-258, 1990.
86. Watson, EE. Marrow dose calculation: Preserit knowledge. Antibody Immunoconjugates, and Radiopharmaceuticals 3(4): 259-262, 1990.
87. Siegel, JA. Direct measurement of activity in bone marrow. Antibody Immunoconjugates, and Radiopharmaceuticals 3(4): 263-264, 1990.
88. Wessels, BW. Direct measurements of bone marrow activity and absorbed dose. Antibody Immunoconjugates, and Radiopharmaceuticals 3(4): 265-268, 1990.
89. Stickney, DR. A method for bone marrow dosimetry. Antibody Immunoconjugates, and Radiopharmaceuticals 3(4): 269-272, 1990.
90. Badger, CC. Bone marrow toxicity for I-131 labeled antibodies. Antibody Immunoconjugates, and Radiopharmaceuticals 3(4) 281-288, 1990.
91. DeNardo GL, DeNardo SJ, Macey DJ, Mills SL: Quantitative pharmacokinetics of radiolabeled monoclonal antibodies for imaging and therapy in patients. In: Radiolabeled Monoclonal Antibodies for Imaging and Therapy - Potential, Problems and Prospects. NATO Advanced Study Institute. S. Srivastava (ed.), Plenum Publishing Co. 1988.
92. DeNardo GL, Macey DJ, DeNardo SJ. Role of absolute quantification of monoclonal antibodies in maging and therapy. Siemens Dialogos Spring/Summer, 2-11, 1990.
93. Hammond ND, Moldofsky PJ, Beardsley MR, Mulhern CB Jr. External imaging techniques for quantitation of distribution of I-131 $F(ab)_2$ fragments of monoclonal antibody in humans. Med Phys 1984: 11:778-783.
94. Griffith, M.H., E.D. Yorke, B.W. Wessels, G. L. DeNardo, W.P. Neacy. Direct dose confirmation of quantitative autoradiography with micro-TLD measurements for radioimmunotherapy. Journal of Nuclear Medicine 29:1795-1809, 1988.
95. Larson, SM, Raubitchek, A, Reynolds JC, Neumann RD, Hellstrom KE, Hellstrom I, Colcher D, Schlom J. Glatstein E, and Carrasquillo JA.: Comparision of bone marrow dosimetry and toxic effect of high dose I-131 labeled monoclonal antibodies administered to man. Int J Radiat Appl Instrum. 16: 153-158, 1989.
96. DeNardo SJ, Macey DJ, DeNardo. A direct approach for determining marrow radiation from MoAb therapy, p. 110-124. In GL DeNardo (Ed.), Biology of Radionuclide Therapy. American College of Nuclear Physicians, Washington, D.C., 1989.
97. Macey, D.J., G.L. DeNardo, S.J. DeNardo. A treatment planning program for radioimmunotherapy, p. 123-131. In J.M. Vaeth (Ed), Frontiers of Radiation Therapy and Oncology: The present and future role of monoclonal antibodies in the management of cancer. Vol. 24, S. Karger AG, Basel, Switzerland, 1990.
98. Deshpande, S.V., S.J. DeNardo, D.L. Kukis, M.K. Moi, M.J. McCall, G.L. DeNardo, C.F. Meares. Yttrium-90 labeled antibody for therapy: Labeling by a macrocyclic bifunctional chelating agent. Journal of Nuclear Medicine 31:473-479, 1990.
99. Adams, G.P., S.J. DeNardo, A. Amin, L.A. Kroger, G.L. DeNardo, I. Hellstrom, K.E. Hellstrom. Comparison of the pharmacokinetics in mice and the biological activity of murine L6 and human-mouse chimeric Ch-L6 antibody. Antibody, Immunoconjugates, and Radiopharmaceuticals, 1991 (In Press).

100. DeNardo, G.L., S.J. DeNardo, K.R. Lamborn, K. Van Hoosear, L.A. Kroger. Enhancement of tumor uptake of monoclonal antibody in nude mice with PEG IL-2. Antibodies, Immunoc...,ugates and Radiopharmaceuticals, 1991 (In Press).

101. DeNardo, G.L., S.J. DeNardo, C.F. Meares, D. Kukis, H. Dirll, M.J. McCall, G.P. Adams, L.F. Mausner, D.C. Moody, S.V. Deshpande. Pharmacokinetics of Copper-67 conjugated Lym-1, a potential therapeutic radioimmunoconjugate, in mice and in patients with lymphoma. Antibodies, Immunoconjugates and Radiopharmaceuticals, 1991 (In Press).

END

DATE
FILMED
4/9/92

I